General Disclaimer

One or more of the Following Statements may affect this Document

- This document has been reproduced from the best copy furnished by the organizational source. It is being released in the interest of making available as much information as possible.

- This document may contain data, which exceeds the sheet parameters. It was furnished in this condition by the organizational source and is the best copy available.

- This document may contain tone-on-tone or color graphs, charts and/or pictures, which have been reproduced in black and white.

- This document is paginated as submitted by the original source.

- Portions of this document are not fully legible due to the historical nature of some of the material. However, it is the best reproduction available from the original submission.

CR 73325

AVAILABLE TO THE PUBLIC

TECHNICAL REPORT

STUDY OF VIBRATIONAL EXCITATION MECHANISMS OF CO_2

J.W. RICH, R.G. REHM, C.E. TREANOR

CAL No. AM-2438-A-1

Prepared for:

National Aeronautics and Space Administration
Ames Research Center
Moffett Field, California

INTERIM REPORT
Contract No. NAS 2 - 4185
October 31, 1968

CORNELL AERONAUTICAL LABORATORY, INC.
OF CORNELL UNIVERSITY, BUFFALO, N. Y. 14221

CORNELL AERONAUTICAL LABORATORY, INC.
Buffalo, New York 14221

Aerodynamic Research Department

STUDY OF VIBRATIONAL EXCITATION MECHANISMS OF CO_2 AT HIGH TEMPERATURES

CAL Report No. AM 2438-A-1
Contract No. NAS 2-4185
October 31, 1968

Prepared for:

National Aeronautics and Space Administration
Ames Research Center
Moffett Field, California

Prepared by: Joseph W. Rich
Joseph W. Rich

Ronald G. Rehm
Ronald G. Rehm

Charles E Treanor
Charles E. Treanor

FOREWORD

The authors would like to acknowledge the assistance of Miss Marcia Williams, who, in addition to programing several of the calculations contained in this report, has provided many helpful suggestions in the course of the work. The programing assistance of Mr. John Moselle is also gratefully acknowledged. This work was supported by the National Aeronautics and Space Administration, Ames Research Center, under Contract NAS 2-4185. The Ames technical monitor was Mr. Robert McKenzie of the Hypersonic Aerodynamics Branch; the Ames contract administrator was Mr. Robert Dolan of the Contract Administration Section.

ABSTRACT

The work presented is an interim report on theoretical studies of CO_2 vibrational relaxation. Major emphasis to date has been placed on obtaining reasonable models for calculating cross sections for the inelastic collision of a structureless particle with a CO_2 molecule. The CO_2 molecule itself is modeled by assuming adiabaticity of the electronic motion, so that the only participating degrees of freedom are the translational modes, and the rotational and vibrational modes of the CO_2 molecule. The analyses reported are either classical or semiclassical in nature. Methods of analysis, such as first order perturbation theory, specifically applicable only at low thermal velocities are avoided.

An empirical approach to the problem of specifying the intermolecular potential is adopted. The intermolecular potential functions chosen have been simple analytical forms, with parameters which can be varied to investigate their influence, or, alternately, matched to available experimental data.

The results of calculations for the vibrational excitation of CO_2, in an approximate normal mode model, are reported. In these calculations, the intermolecular potential is not spherically symmetric, allowing investigation of the effects of potential anisotropy and participation of the rotational energy mode. It is found that the rotational mode can make a contribution to vibrational excitation over a considerable range of relative translational energies in the collision. The degree of participation of the rotational mode is a strong function of the potential anisotropy.

A discussion is given of a Monte Carlo scheme for obtaining thermally-averaged cross sections for vibrational excitation. The scheme utilizes the variance reducing technique of importance sampling, together with a property of averaging integrals, to calculate the integrals for several temperatures efficiently.

Completely analytical studies of greatly simplified models of the collision process also are reported. In particular, an approximate model of potential anisotropy and rotational effects is given. An analytical form for the vibrational

energy gained by the vibrational mode during collision is obtained.

Model analyses currently in progress also are outlined. These analyses include a complete classical treatment for CO_2-M collisions, and a semi-classical treatment which includes the effect of anharmonicity coupling among the CO_2 vibrational modes.

TABLE OF CONTENTS

Section		Page
	FOREWORD	ii
	ABSTRACT	iii
	TABLE OF CONTENTS	v
	LIST OF ILLUSTRATIONS	vi
1.	INTRODUCTION	1
2.	DECOUPLED, NORMAL-MODE MODEL OF CO_2 - M COLLISIONS	4
3.	MONTE CARLO CALCULATIONS	24
4.	FOUR-BODY CLASSICAL DESCRIPTION OF CO_2 - M COLLISIONS	31
5.	ANALYTICAL STUDIES	41
6.	INTERMODE COUPLING MODEL	61
7.	SUMMARY	69
	APPENDIX A	73
	APPENDIX B	77
	REFERENCES	79

LIST OF ILLUSTRATIONS

Figure		Page
1.	Scattering Coordinates	5
2.	Molecular Orientation	5
3.	Normal Modes	7
4.	CO_2-Ar ΔE_v for Symmetric Stretching Mode	15
5.	CO_2-Ar ΔE_v for Bending Mode	15
6.	CO_2-Ar ΔE_v for Asymmetric Stretching Mode	16
7.	Classical Energy Transferred to CO_2 ν_1 Mode in Collision with Ar vs. Impact Parameter	18
8.	Classical Energy Transferred to CO_2 ν_2 Mode in Collision with Ar vs. Impact Parameter	19
9.	Classical Energy Transferred to CO_2 ν_3 Mode in Collision with Ar vs. Impact Parameter	20
10.	Molecule-Atom Coordinates	25
11.	Initial Trajectory Orientation	25
12.	Complete Classical Description-Coordinate System	35
13.	Classical Energy ΔE_v Transferred to Symmetric Stretching Mode of CO_2 During Collision with Ar , as a Function of Collision Energy.	47
14.	Classical Energy ΔE_v Transferred to Symmetric Stretching Mode of CO_2 During Collision with Ar , as a Function of Collision Energy	47
15.	Classical Energy ΔE_v Transferred to Vibrational Mode of O_2 During Collision with Ar , as a Function of Translational Energy	49
16.	Classical Energy ΔE_v Transferred to Vibrational Mode of O_2 During Collision with Ar , as a Function of $(E_T + E_{ROT})^{-1/2}$	50
17.	Classical Energy ΔE_v Transferred to Vibrational Mode of O_2 During Collision with Ar , as a Function of Impact Parameter	52
18.	ΔE_v Transferred to Symmetric Stretching Mode of CO_2 During Collision with Ar	53

Figure		Page
19.	CO_2 Asymmetric Stretching Mode. Critical Velocities vs. Temperature	56
20.	CO_2 Bending Mode. Critical Velocities vs. Temperature	57
21.	CO_2 Asymmetric Stretching Mode. V-T Non-Perturbative Transition Probabilities	59
22.	CO_2 Bending Mode. V-T Non-Perturbative Transition Probabilities	60
23.	CO_2 Energy Levels	64

1. INTRODUCTION

Vibrational relaxation in gases is a nonequilibrium process that has received extensive theoretical and experimental study in recent years. Interest has been occasioned by the importance of this process in high temperature gas flows, in many chemical reactions, and, most recently, in molecular gas lasers. The understanding and prediction of vibrational relaxation mechanisms in CO_2, in particular, is necessary both for analysis of the gas dynamic phenomena occurring upon entry into planetary atmospheres and for performance analysis of CO_2 gas lasers.

The work presented in this report is a theoretical study of CO_2 vibrational relaxation. Major emphasis to date has been placed on obtaining reasonable models for calculating cross sections for the inelastic collision of a structureless particle with a CO_2 molecule. The CO_2 molecule itself is modeled by assuming adiabaticity of the electronic motion, so that the only degrees of freedom are the translational modes, and the rotational and vibrational modes of the CO_2 molecule. The remaining paragraphs of this introduction outline, in more detail, some of the considerations entering into the present study.

Considerable progress[1-9] has been made in the calculation of cross sections for vibrational energy excitation in nonpolar diatomic molecules, and in prediction of the overall vibrational relaxation times for such species. It has been shown, however, that a major problem in these calculations is the extreme sensitivity of the cross sections to potential details, particularly at low thermal velocities (Ref 10, pgs. 685-691). In order to predict accurately the absolute magnitude of the cross section for an inelastic event of this type, the inter- and intramolecular potential functions must be known accurately. Little is known, however, of the intermolecular potential function for CO_2, other than what is available from measurements of virial coefficients. Any choice of a potential function must be regarded as postulational. One requires either detailed molecular scattering experiments or elaborate large-scale quantum mechanical potential calculations in order to establish, ab initio,

the correct potential. In the absence of such investigations, the present study adopts an empirical approach to the problem of specifying the intermolecular potential. The intermolecular potential functions chosen have been simple, analytical forms, with parameters which can be varied to investigate their influence, or, alternately, matched to available experimental data.

As general a treatment as possible was desired. In particular, we have attempted to model those features which distinguish CO_2, a linear triatomic, from the more commonly studied diatomic case. Such features include a more marked departure from spherical symmetry, the influence of the vibrational bending modes, and intermode coupling within the molecule. Several theoretical treatments of CO_2 vibrational relaxation are already extant.[11-14] However, each of them possesses at least one of the following limitations:

1. Restriction to a first order perturbation approximation.[11, 13, 14]
2. Neglect of intermode coupling effects within the CO_2 molecule.[12, 13, 14]
3. Neglect of molecular rotation effects and potential anisotropy.[11, 12, 13]

The models and analysis discussed in this report are directed toward removal of these restrictions.

The analyses presented in the subsequent sections are classical or semiclassical in nature. It can be noted that, in recent years, completely classical models have been used to calculate numerically both vibrational energy transfer cross sections[4, 15] and reactive scattering cross sections[16, 17] in simple molecules. The reactive scattering calculations, in particular, have met with considerable success in interpreting molecular beam reactive scattering experiments. A completely classical model for CO_2 collisions is presented in Section 4 of this report. However, most of the studies contained herein are semiclassical; retention of a quantum-mechanical description of the vibrational modes was felt to be desirable for analyzing vibrational processes in CO_2. The quantized nature of the vibrational-energy modes of CO_2 is emphasized by the techniques and phenomena of experimental

studies. One example is afforded by recent experiments[18, 19] in which a vibrational fluorescence technique is used to study the collisional deactivation of the first excited state of the asymmetric stretching vibration (00°1) of CO_2 in rare-gas diluents. It appears that this deactivation proceeds by mean of intramolecular vibration-to-vibration energy transfer during CO_2 rare-gas collisions. It is found that these results can be interpreted only if Fermi resonance and Coriolis mixing of the CO_2 vibrational states is considered. A second example is the analysis of the behavior and performance of CO_2 infrared lasers.[20] Application of theory to such processes makes a quantum mechanical treatment of the vibrational states extremely desirable.

Finally, it should be mentioned that it is desired to apply the theory developed in this study over a wide range of kinetic temperature. Thus methods of analysis specifically applicable only at low thermal velocities, such as first order perturbation theory, are avoided.

The remainder of the report is in five sections plus appendices. Section 2 presents an analysis of a normal mode model for CO_2-M collisions. The approximations introduced in this analysis make it appropriate for calculation of the rate for direct translation-to-vibration thermal excitation of CO_2. Molecular rotational effects are included. Section 3 outlines a Monte Carlo procedure for the averaging of the cross sections obtained in Section 2 over a thermal distribution of trajectory parameters. Section 4 gives a more exact, completely classical analysis of CO_2-M collisions. It is planned to make some limited numerical calculations on the basis of this analysis to assess the accuracy of the approximations introduced in the theory of Section 2. The work in Sections 2 - 4 depends greatly on machine computation. In Section 5, completely analytical studies of greatly simplified models of the vibrational excitation process are discussed. These analytical studies were undertaken both to provide a guide for the more exact numerical computations and to gain additional insight into certain specific aspects of the overall problem. The concluding Section, 6, gives a model for calculating collision-induced energy transfer processes among the various coupled vibrational modes of the CO_2 molecule.

2. DECOUPLED, NORMAL-MODE MODEL OF CO_2-M COLLISIONS

2.1 COORDINATE SYSTEM

We consider the collision of the CO_2 molecule with another molecule, which has been assumed to possess no internal modes, i.e., to be a structureless point-mass type particle. Only the nuclear motion of the CO_2 molecule is specifically considered. No electronic excitation is treated. We therefore have what is essentially a four-body problem. For our purposes, the energy of such a system can be expressed conveniently as the sum of the following terms:

1. The kinetic energy of translation of the center of mass of the entire molecule-particle system.

2. The kinetic energy of the incident particle and the molecule relative to their center of mass.

3. The kinetic energy of the molecule's atoms relative to the molecular center of mass.

4. The internal potential energy of the molecule.

5. The potential energy arising from the interaction of the incident particle with the molecule.

In the standard fashion, the kinetic energy term (1) can be ignored, using center-of-mass coordinates, since there is no potential affecting the entire system. We therefore consider a system of space-oriented coordinates x, y, z with origin at the center of mass of the molecule.

The position of the incident particle relative to the scattering center can be described in terms of the standard scattering coordinates (R, Θ, Φ) or $\bar{R}$, as indicated in Fig. 1. The time variation of $\bar{R}$ determines term 2 above.

The problem of describing the internal energy of the CO_2 molecule (terms 3 and 4) is more complex. In the present section, the normal-mode

approximation of the CO_2 internal energy is used. (More general considerations are treated in Sections 4 and 6.) For the present purpose, the coordinate system is shown in Fig. 2. Figure 2 illustrates the relation between a coordinate system ($x' y' z'$) fixed in the molecule and the previously introduced xyz system. As shown in the figure, the z' axis is the molecular axis, i.e., the line of nuclear centers in the equilibrium configuration of the linear triatomic molecule.

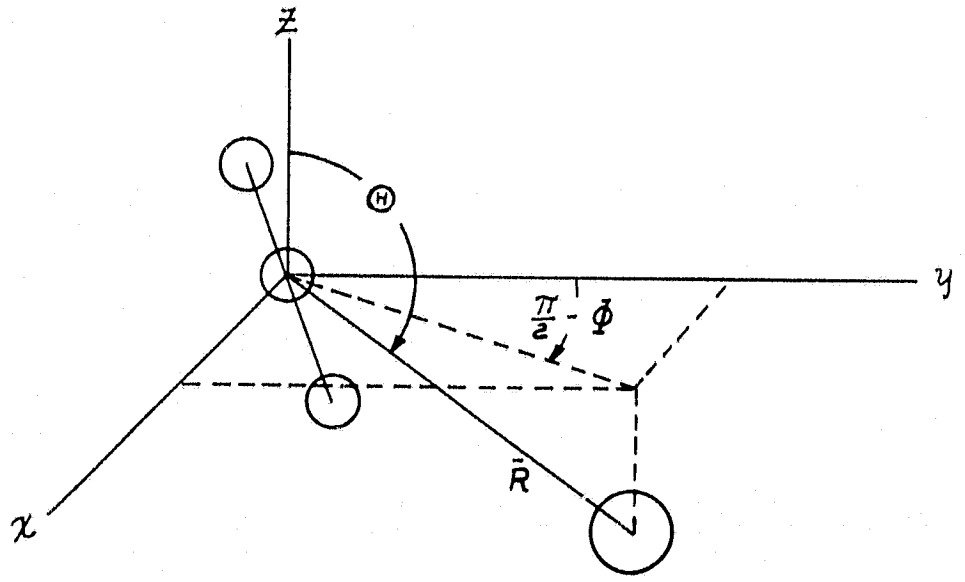

Fig. 1

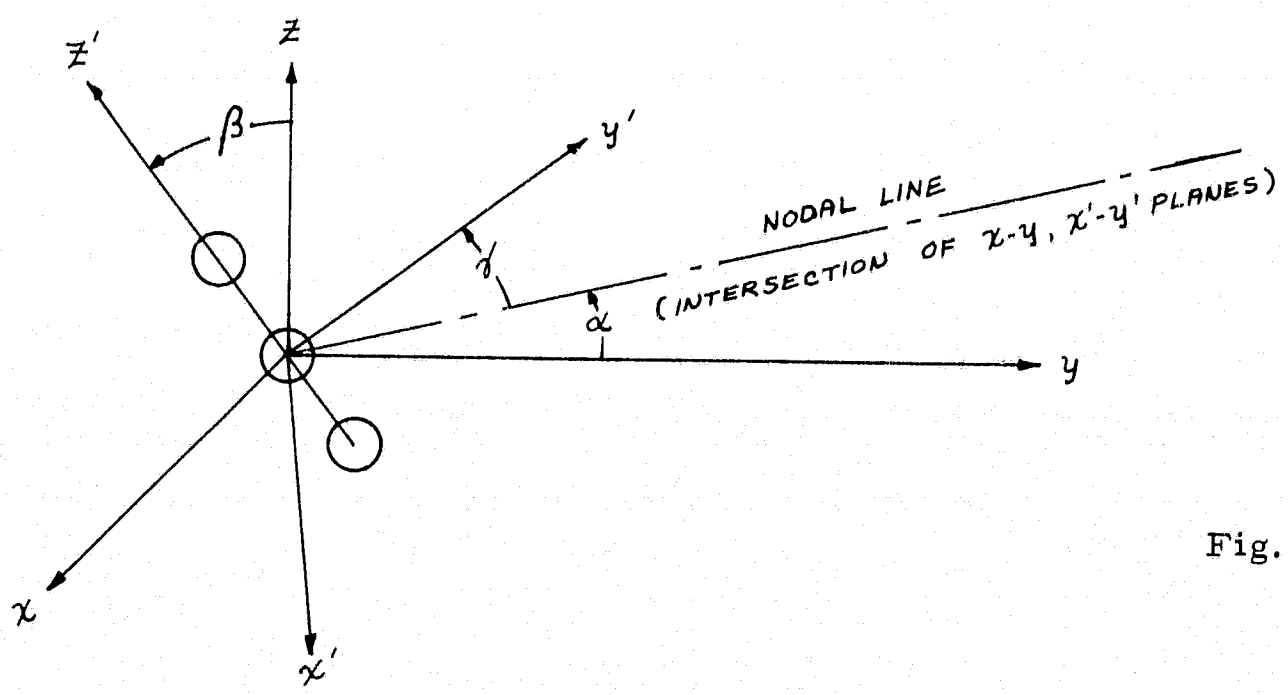

Fig. 2

The χ'-z' plane is defined as the plane of the bending motion of the molecule. α, β, γ are the Euler angles according to the convention of Rose,[21] which give the instantaneous orientation of the primed system with respect to the unprimed system. In the present case, α and β are actually the azimuthal and polar angles defining the location of the equilibrium molecular axis. γ specifies the orientation of the CO_2 bending plane about this axis. If $\bar{R}$ is a vector in the unprimed system, it is expressed in the primed system through the rotation matrix A ,

$$\bar{R}' = A\bar{R},$$

where

$$A = \begin{pmatrix} [\cos\alpha\cos\beta\cos\gamma - \sin\alpha\sin\beta] & [\sin\alpha\cos\beta\cos\gamma + \cos\alpha\sin\gamma] & -\sin\beta\cos\gamma \\ -[\cos\alpha\cos\beta\sin\gamma + \sin\alpha\cos\gamma] & [-\sin\alpha\cos\beta\sin\gamma + \cos\alpha\cos\gamma] & \sin\beta\sin\gamma \\ \cos\alpha\sin\beta & \sin\alpha\cos\beta & \cos\beta \end{pmatrix} \tag{2-1}$$

2.2 SYSTEM HAMILTONIAN

The total Hamiltonian, disregarding the system mass motion, is written as the sum of the last four contributions listed in Section 2.1:
They are specified in turn here:

I. Incident particle kinetic energy (term 2):

$$H_a = \frac{1}{2MR^2}\left(R^2 P_R^2 + P_\Theta^2 + \sin^{-2}\Theta\, P_\Phi^2\right), \tag{2-2}$$

$$P_R = M\dot{R}, \qquad P_\Theta = MR^2\dot{\Theta}, \qquad P_\Phi = MR^2\sin^2\Theta\,\dot{\Phi}$$

II. Internal kinetic and potential energy of the CO_2 molecule (terms 3 and 4):

As mentioned above, a normal mode approximation to the CO_2 internal energy states is adopted in this section. The direction of the normal vibrational

displacements, using the notation of Herzberg[22] is given in Fig. 3:

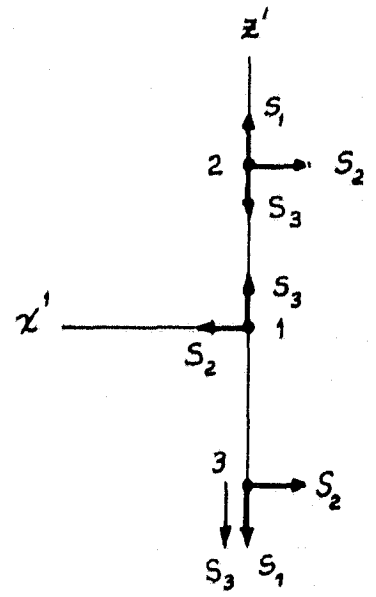

Fig. 3

Then

$$H_M = \frac{1}{2} d_{11} \dot{S}_1 + \frac{1}{2} d_{22} (\dot{S}_2^2 + S_2^2 \dot{\gamma}^2) + \frac{1}{2} d_{33} \dot{S}_3^2$$

$$+ \frac{1}{2I} (P_\beta^2 + \sin^{-2}\beta P_\alpha^2)$$

$$+ \frac{1}{2} C_{11} S_1^2 + \frac{1}{2} C_{22} S_2^2 + \frac{1}{2} C_{33} S_3^2 \quad ,$$

$$P_\beta = I \dot{\beta} , \qquad P_\alpha = I \dot{\alpha} \sin^2\beta$$

(2-3)

Here

$$d_{11} = 2m_o , \quad d_{22} = m_c + \frac{m_c^2}{2m_o} , \quad d_{33} = m_c + \frac{m_c^2}{2m_o} ,$$

$$C_{11} = 2(a_{11} + a_{12}) , \quad C_{22} = a_{33} \frac{4(1+\mu)^2}{l^2} , \quad C_{33} = 2(1+\mu)^2 (a_{11} - a_{12}) ,$$

where $\mu = m_c / 2m_o$ and a_{11} is the force constant of the C-O bond (ergs cm^{-2}), a_{12} is the force constant that gives the interaction of the two C-O bonds (ergs cm^{-2}), and a_{33} (ergs rad^{-2}) is the force constant for the

bending of the molecule.[22]

In the above expression for H_m , the terms in the first line are the kinetic energy associated with vibration; the terms in the second line are the kinetic energy of molecular (rigid rotator) rotation; and the last line represents the potential energy (harmonic motion approximation). S_1 is the coordinate for the symmetric stretching mode. S_2 and γ are the coordinates of normal displacement due to bending. It should be recalled that the third Eulerian angle, γ , corresponds to a rotation about the z' (molecular) axis; the terms in S_2 and γ are the energy for a two-dimensional isotropic harmonic oscillator, expressed in polar coordinates. S_3 is the coordinate for the asymmetric stretching mode.

The Hamiltonian given by Eq (2-3) omits terms coupling the vibrational modes, such as created by anharmonicity. Further, terms coupling the rotational and vibrational motions, created by Coriolis and centrifugal forces, also are neglected. Finally, small amplitude bending is assumed, and therefore the Hamiltonian for a rigid rotator is used, rather than the much more complex general rotational operator.

III. Intermolecular Potential Energy (term 5):

We take this potential to be a linear combination of three point-center interactions

$$V(r_i) = \sum_{i=1}^{3} V_i(r_i) \qquad (2-4)$$

For the purposes of discussion, it is assumed that r_i represents the distance from the incident particle to the i^{th} nucleus of the CO_2 molecule. However, as will be discussed below, the resulting potential can be parametrically varied to account for interactions not centered on the nuclei.

We have chosen, for the V_i , simple exponential interactions. In particular, for V_1 , the potential centered on the carbon nucleus, we choose a linear combination of attractive and repulsive exponentials

$$V_1 = C_1 e^{-\alpha_1 r_1} - C_4 e^{-\alpha_4 r_1} \qquad (2-5a)$$

For V_2, V_3 simple exponential repulsive interactions are taken

$$V_2 = C_2 e^{-\alpha_2 r_2}, \qquad V_3 = C_3 e^{-\alpha_3 r_3} \tag{2-5b, 5c}$$

The distances r_i can be written in terms of the coordinates of Figs. 1 and 2. Further, the cartesian coordinates of the vibrational displacements can be expressed in terms of the normal displacements of Fig. 3, using the geometrical relationships of Fig. 2 and the rotation matrix A. The complete result is somewhat cumbersome, and will not be quoted here. However, if, following Takayanagi,[8] we expand the potential Eq (2-4) about the equilibrium positions of the nuclei, and retain only terms to first order in the ratio of the vibrational displacements to R, a basic ordering in the potential terms can be observed. Finally, the result may be further simplified if we neglect ℓ^2/R^2 compared with 1, where ℓ is the equilibrium C-O separation. This gives a result corresponding to the first term in an expansion of the potential about the spherically symmetric case only. The result of this procedure will be quoted:

$$V = C_1 e^{-\alpha_1 R} - C_4 e^{-\alpha_4 R} + 2 C_2 e^{-\alpha_2 R} \cosh(\alpha_2 \ell \cos\Theta') + \sum_{i=1}^{3} f_i S_i , \tag{2-6}$$

where

$$f_1 = -2 C_2 \alpha_2 e^{-\alpha_2 R} \left[\left(\frac{\ell}{R}\right) \cosh(\alpha_2 \ell \cos\Theta') + \cos\Theta' \sinh(\alpha_2 \ell \cos\Theta') \right]$$

$$f_2 = -\left[C_1 \alpha_1 e^{-\alpha_1 R} - C_4 \alpha_4 e^{-\alpha_4 R} + 2 C_2 \alpha_2 e^{-\alpha_2 R} \frac{m_c}{2m_o} \cosh(\alpha_2 \ell \cos\Theta') \right]$$
$$\left[\cos\beta \cos\gamma \sin\Theta \cos(\alpha - \Phi) - \sin\beta \cos\gamma \cos\Theta - \sin\gamma \sin\Theta \sin(\alpha - \Phi) \right]$$

$$f_3 = -(C_1 \alpha_1 e^{-\alpha_1 R} - C_4 \alpha_4 e^{-\alpha_4 R}) \cos\Theta'$$
$$+ 2 C_2 \alpha_2 e^{-\alpha_2 R} \frac{m_c}{2m_o} \left[\cos\Theta' \cosh(\alpha_2 \ell \cos\Theta') - \frac{\ell}{R} \sinh(\alpha_2 \ell \cos\Theta') \right]$$

(2-7a, b, c)

Here, Θ' is the angle between $\bar{R}$ and the molecular axis:

$$\cos\Theta' = \cos\beta\cos\Theta - \sin\alpha\sin\Theta\sin(\beta-\phi) \tag{2-8}$$

The first two terms in this potential cause purely elastic scattering, being functions of the translational coordinate only. The third term gives rise to rotational transitions, while the remaining terms create simultaneous rotational-vibrational transitions. It is seen that rotational excitation can be treated independently of vibrational excitation, but if one retains the effect of vibrational structure in the potential, one must also treat rotational interactions to maintain a consistent level of approximation.

The first three terms in this potential are similar to the potential adopted by Parker[23] to calculate rotational relaxation times for diatomic molecules. Parker, however, did not require all his potentials to be centered on the nuclei but allowed the 2, 3 potential centers to be closer to the mass center along the molecular axis to account for the repulsive interaction of the electron cloud. This procedure corresponds to letting ℓ in Eq (2-6) be a variable parameter which can be less than the equilibrium C-O separation. Raff[24] has shown that the procedure gives rotational excitation cross sections which can be in good agreement with calculations based on more exactly determined potentials for simple systems such as H_2 - He . Thus, although it is acknowledged that pairwise potentials, such as Eq (2-5), centered on the nuclei, are not entirely satisfactory, one can approximate the true potential by letting ℓ be a variable parameter.

The total Hamiltonian is the sum of Eqs (2-2), (2-3), and (2-6):

$$H = H_a + H_m + V \tag{2-9}$$

2.3 METHOD OF SOLUTION OF EQUATIONS OF MOTION - THE DECOUPLING APPROXIMATION

The approximate Hamiltonian (2-9) developed above leads to equations of motion for the CO_2-M system which are still quite complex. In particular, the three energy modes: vibration, rotation, and translation, are coupled through the intermolecular potential function V . We are principally interested

in calculating the rate of excitation of the vibrational modes by energy transfer from the "external modes" of rotation and translation. To facilitate such calculation, an additional approximation is adopted. The last terms in Eq (2-6) for the potential, $\sum_i f_i S_i$, are neglected. This implies a neglect of the influence of molecular vibrations on the translational and rotational motion of the system. The equations of motion are then merely those governing the collision of an atom and a (triatomic) rigid rotator, under the influence of the pairwise exponential intermolecular potentials previously given.* These equations can be solved numerically on a machine, to obtain the time variation of the trajectory parameters R , Θ , Φ , α , β during the course of a CO_2-M collision.

Having obtained $R(t)$, $\Theta(t)$ etc, one can regard the coefficients f_i in the previously neglected potential term $\sum_i f_i S_i$ as functions of time only, $f_i(t)$. With this approximation, the equations governing the vibrational motion are separable, and all are of the form**:

$$d_{ii} \ddot{S}_i + C_{ii} S_i = f_i(t) \qquad (2\text{-}10)$$

It is a known result[25] that use of the solution of Eqs (2-10) gives energy transferred to the i^{th} vibrational mode to be:

$$\Delta E_{v_i} = \frac{1}{2d_{ii}} \left| \int_{-\infty}^{\infty} f_i(t') e^{i\omega_{v_i} t'} dt \right|^2 , \qquad (2\text{-}11)$$

where $\omega_{v_i} = (C_{ii}/d_{ii})^{1/2}$ is the radial vibrational frequency of the i^{th} mode.

We again emphasize that $f_i(t)$ is known as a result of the classical trajectory solutions, since $R(t)$, $\Theta(t)$ ....etc. are obtained from the trajectory

---

* The actual classical trajectory equations as programed are given in Appendix A.

** Some manipulation is necessary to achieve this result for the bending mode coordinates. Putting $S_{2a} = S_2 \sin\gamma$, $S_{2b} = S_{2b} \cos\gamma$, separation is possible; one obtains $d_{22} \ddot{S}_{2a} + C_{22} S_{2a} = f_{2a}(t)$, $d_{22} \ddot{S}_{2b} + C_{22} S_{2b} = f_{2b}(t)$, where the forcing functions f_{2a} and f_{2b} are such that $f_{2a} S_{2a} + f_{2b} S_{2b} \equiv f_2 S_2$.

calculations, and f_i is an explicit function of these trajectory parameters.

One of the problems in this formalism is the evaluation of the "perturbation integral,"

$$J = \int_{-\infty}^{\infty} f_i(t)\, e^{i\omega_{v_i} t'}\, dt' \qquad (2\text{-}12)$$

The numerical evaluation of this expression has long been recognized as a nontrivial task, due to the oscillatory nature of the integrand.[26] This difficulty is compounded in the present case wherein $f_i(t)$ may itself have an oscillatory component due to molecular rotation.* In the present study, these integrals are programed for calculations simultaneously with the trajectory calculations discussed in the preceding paragraphs. A Runge-Kutta routine is used.

With the preceding method, the energy transferred to the i^{th} vibrational mode of the CO_2 molecule, ΔE_{v_i}, during a collision with the structureless particle M, can be calculated. The ΔE_{v_i} so calculated is a function of the initial trajectory parameters, which can be conveniently specified as: the initial relative CO_2-M translational velocity, V_∞; the impact parameter b; the initial CO_2 molecular orientation, α_o and β_o, and the initial CO_2 rotational velocity, ω_{α_o} and ω_{β_o}.** Thus, in general,

$$\Delta E_{v_i} = \Delta E_{v_i}(V_\infty, b, \alpha_o, \beta_o, \omega_{\alpha_o}, \omega_{\beta_o})$$

---

* The problem exists even if the decoupling approximation is not introduced in the classical equations. The numerical difficulty then arises when accurately integrating certain of the equations of motion, rather than occurring in the separated integral (2-12).

** The result has already been averaged over the vibrational phase. The ability to do this independently of the trajectory details is a consequence of the decoupling approximation. This same approximation also makes the result independent of the initial vibrational state of the molecule.

2.4 SEMICLASSICAL CALCULATION OF VIBRATIONAL TRANSITION PROBABILITIES

The procedure outlined in the preceding sections leads to the calculation of ΔE_{v_i}, the classical energy gained by the i^{th} CO_2 normal vibrational mode during a collision. In this normal mode model, ΔE_{v_i} is simply the energy acquired by a harmonic oscillator subject to a time-dependent forcing function ($f_i(t)$) representing the effect of the collision. It has been shown[3,27] that if one chooses to adopt a quantum-mechanical description of the harmonic motion of the CO_2 vibrational modes, the ΔE_{v_i}'s are analytically related to the probabilities for transitions among the quantized vibrational states. Specifically, Ref 3 shows that if ΔE_{v_i} is the classical energy transferred during collision to the i^{th} vibrational mode, the probability P^i_{mn} for transition between the m and n^{th} vibrational states of that mode is:

$$P^i_{mn} = m!\, n!\, e^{-\epsilon_i}\, \epsilon_i^{m+n} \left[\sum_{j=0}^{\mu} \frac{(-1)^j\, \epsilon_i^{2j}}{(n-j)!\, j!\, (m-j)!} \right] \qquad (2\text{-}13)$$

where

$\epsilon_i = \Delta E_{v_i} / h\nu_i$

ν_i = frequency of i^{th} mode

μ = lesser of m, n

It should be noted that the adoption of a normal mode model and use of the potential (V) linearized in the vibrational displacements prevents any coupling between modes. The model used in this section is directed towards a calculation of the rate of vibrational excitation via energy transfer from the translational and rotational modes (see the following section). Section 6 outlines a model which specifically treats the problem of CO_2-M collisions with coupled vibrational modes.

A second feature of the transition probability given in Eq (2-13), is that it is an exact result for a linearly forced harmonic oscillator. In the limit of small energy transfer, $\epsilon_i << 1$, it can be shown that Eq (2-13) reduces to the perturbation result given by a first order time dependent perturbation analysis or a distorted wave treatment. For example, in this limit,

$$P^i_{m,m-1} \sim m\,\epsilon_i \qquad \text{for} \qquad \epsilon_i << 1$$

2.5 RESULTS AND DISCUSSION

Numerical computations for the vibrational energy ΔE_{V_i} transferred to each of the three normal modes ($i = 1, 2, 3$) of the CO_2 molecule have been performed. Figures 4-9 show ΔE_{V_i} as calculated with the decoupled normal mode model, as a function of various trajectory parameters. The results in these figures are for coplanar cases, for which $\beta = \pi/2$ and $\omega_{\beta_0} = 0$, although the programs also can treat the general three-dimensional case. The ΔE_{V_i}'s have been numerically averaged over the initial rotational phase (α orientation). Thus the ΔE_{V_i}'s shown in the figures are functions of the three remaining trajectory parameters: V_∞ , ω_{α_0} & b .

Figures 4-6 show ΔE_{V_i} plotted versus $E_T / h\nu_i$ where $E_T = \frac{1}{2} M V_\infty^2$ is the initial relative translational energy and ν_i is the symmetric stretching mode frequency. These curves are for an impact parameter $b = 0$. Figures 4, 5, and 6 are for the excitation of the symmetric stretching ($i = 1$), bending ($i = 2$) and asymmetric stretching ($i = 3$) modes, respectively. The curves are plotted for varying initial molecular rotational velocities ($\omega_{\alpha_0} = 8.60 \times 10^{11}$, 4.39×10^{12}, 2.01×10^{13}, 3.02×10^{13} rad/sec, which respectively correspond to initial molecular rotational energy $E_R / h\nu_1 = \frac{1}{2} I \omega_{\alpha_0}^2 / h\nu_1 = 0.01$, 0.26, 5.46, 12.3). As is to be expected from adiabalicity considerations, for any given value of E_T and E_R , ΔE_{V_i} is greatest for the softest mode. Thus for given E_T and E_R , $\Delta E_{V_2} > \Delta E_{V_1} > \Delta E_{V_3}$. (The molecular parameters used in preparing these curves are values for CO_2-Ar collisions, taken by matching the Morse potential of Eq (2-5a) to the Lennard-Jones viscosity parameters tabulated in Ref 28. The value of ℓ , the anisotropy parameter, is taken equal to the equilibrium C-O distance.)

The curves also show the effect of molecular rotation. At a given value of E_T , the calculated ΔE_V increases with increasing rotational energy, E_R . This effect of molecular rotation is greater for the lower translational energies, $E_T < E_R$. As E_T exceeds E_R , the translational and rotational modes begin to contribute approximately equally to ΔE_V . These effects of molecular rotation also have been observed in the exact classical machine solution of Benson and Berend,[4] and Kuksenko and Losev.[15] It should be

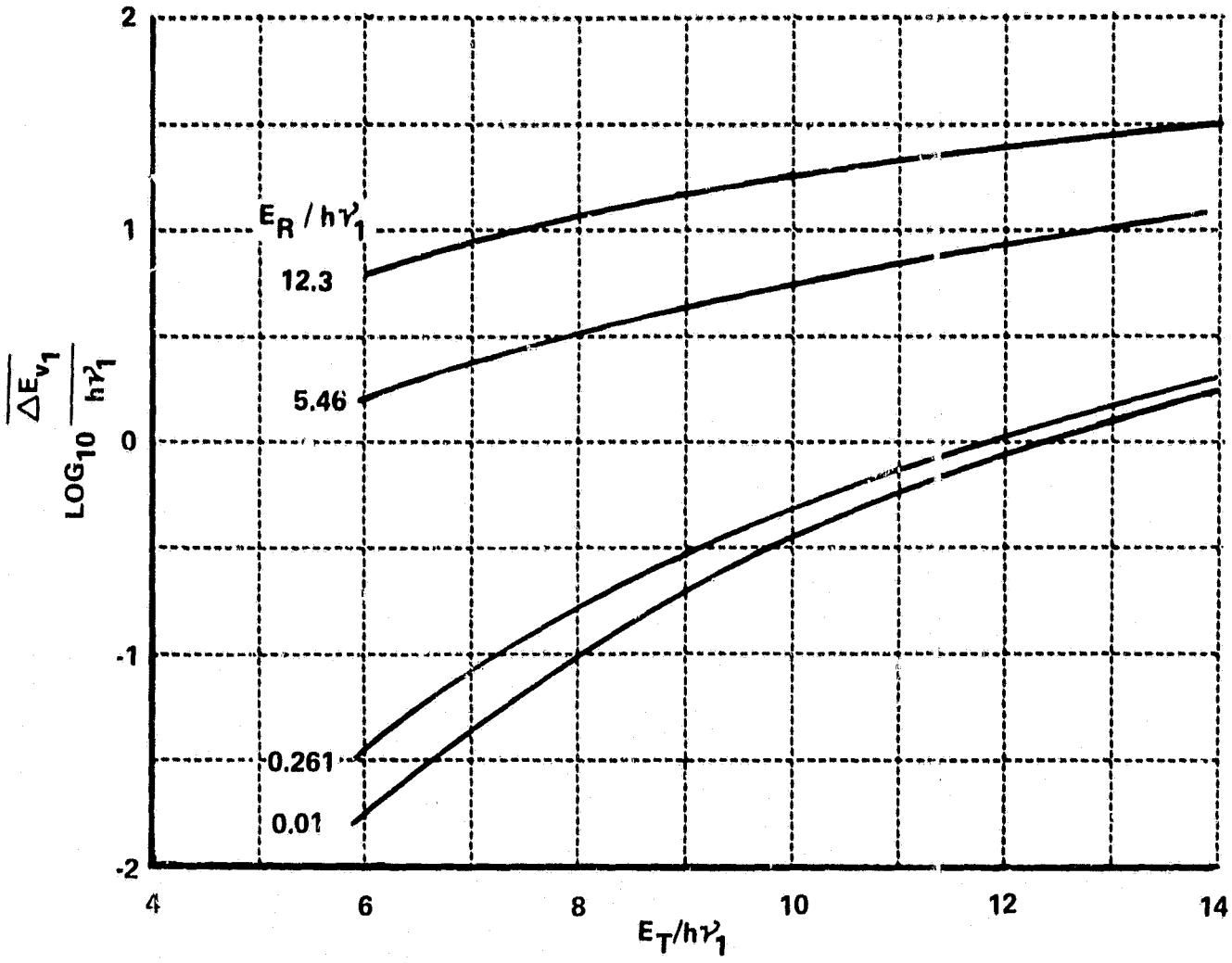

Figure 4 CO_2 - Ar – ΔE_v FOR SYMMETRIC STRETCHING MODE

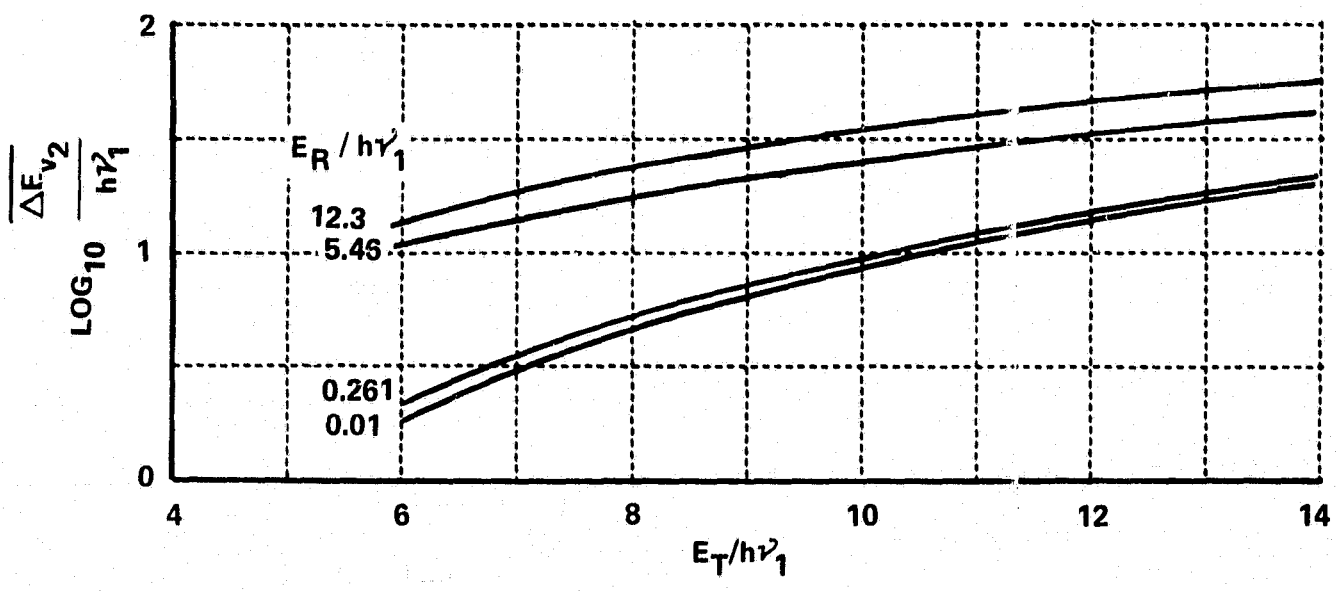

Figure 5 CO_2 - Ar – ΔE_v FOR BENDING MODE

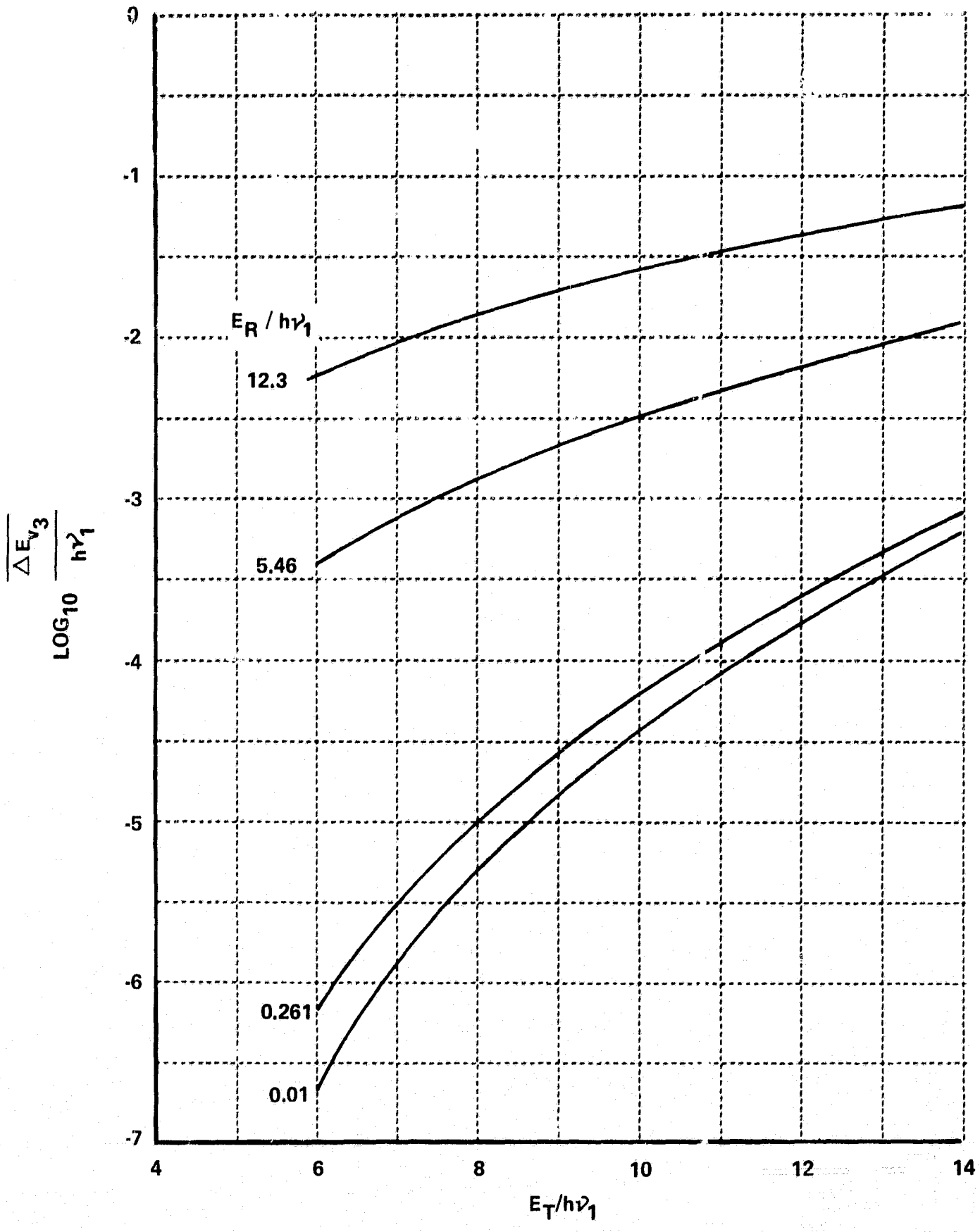

Figure 6 CO_2 - Ar – ΔE_v FOR ASYMMETRIC STRETCHING MODE

remarked that the actual extent of rotational effects is a strong function of the degree of anisotropy in the intermolecular potential function (i.e., the ℓ parameter in Eq (2-6)).*

Dependence of the calculated ΔE_v's on impact parameter is shown in Figs. 7-9, for each of the three modes. The fall-off with b is greater for the stiffer modes.

We conclude this section with a further discussion of the advantages and limitations of the present model.

One of the motivations for the present study was the desire to examine the rate of excitation of the CO_2 vibrational energy states behind strong shock waves. Such a process involves transfer of energy between the rapidly equilibrated "external" modes of translation and rotation, on the one hand, and the vibrational mode on the other. This transfer is called a V-T process. Therefore, the transition probabilities $P^{i}_{m\,n}$ will be averaged over a thermal distribution of the trajectory parameters (V_∞ , b , ω_{α_o} , ω_{β_o} , α_o , β_o) to obtain thermally averaged cross sections for the V-T vibrational excitation process. (A method for performing such a calculation is given in Section 3.) As discussed in the introduction, any empirically chosen intermolecular potential function, such as Eq (2-5), can only be treated as a postulate. Experimental correlations will involve parametric investigation of the dependence of the thermally averaged cross sections on the potential constants.

A principal advantage of the decoupled, normal mode calculations described in this section is that they lend themselves to parametric studies of the intermolecular potential functions used in obtaining the basic V-T relaxation rate for CO_2 . All experimental evidence points to rapid equilibration of energy among the CO_2 normal modes, up to high temperatures. (It is likely that current theoretical examination of intermode energy transfer (Section 6) will support this rapid equilibration model.) Under such conditions

* Further discussion of the effect of potential anisotropy and molecular rotation is given in connection with analytical studies of Section 5.

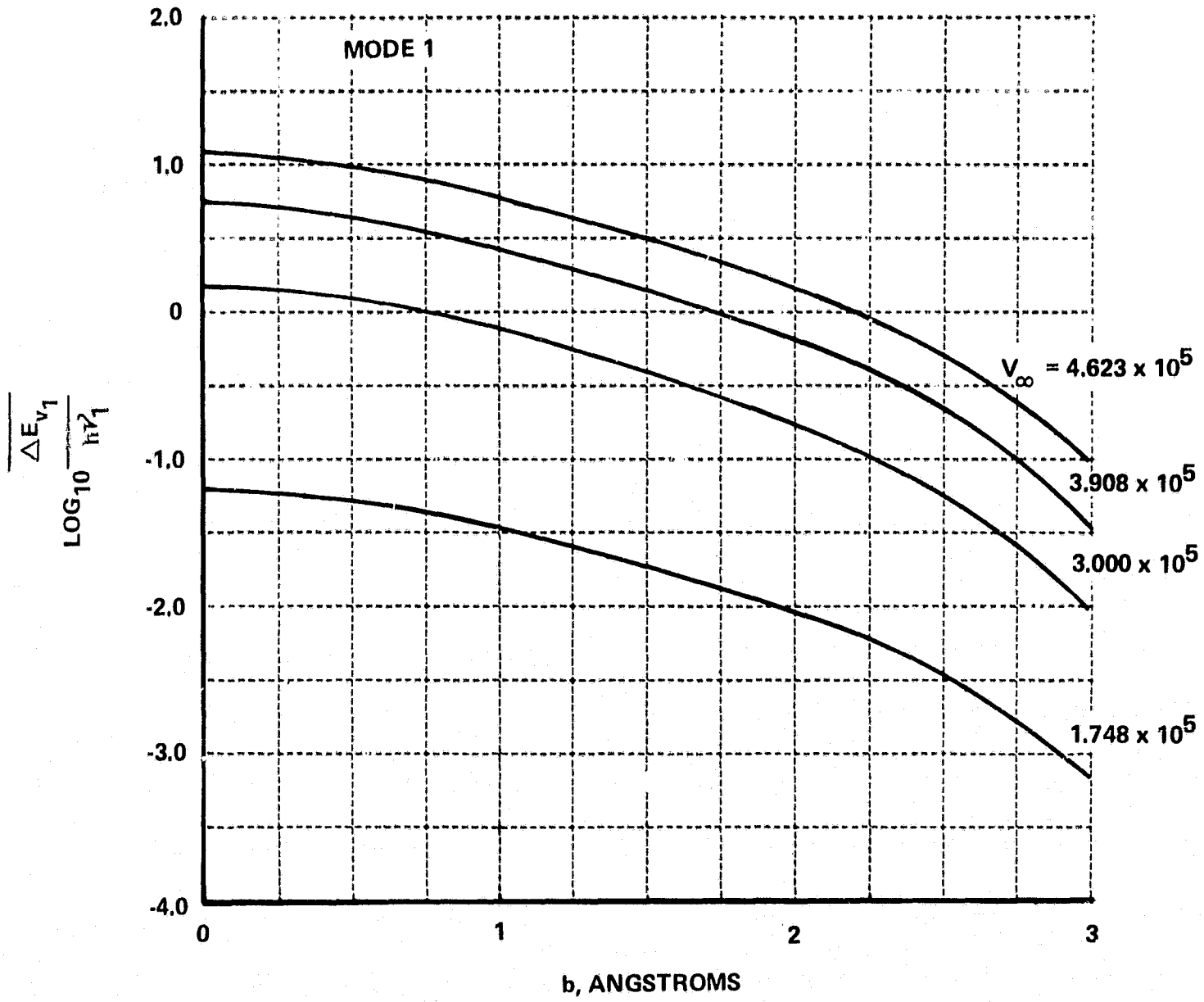

Figure 7 CLASSICAL ENERGY TRANSFERRED TO CO_2 ν_1 MODE IN COLLISION WITH Ar VS. IMPACT PARAMETER

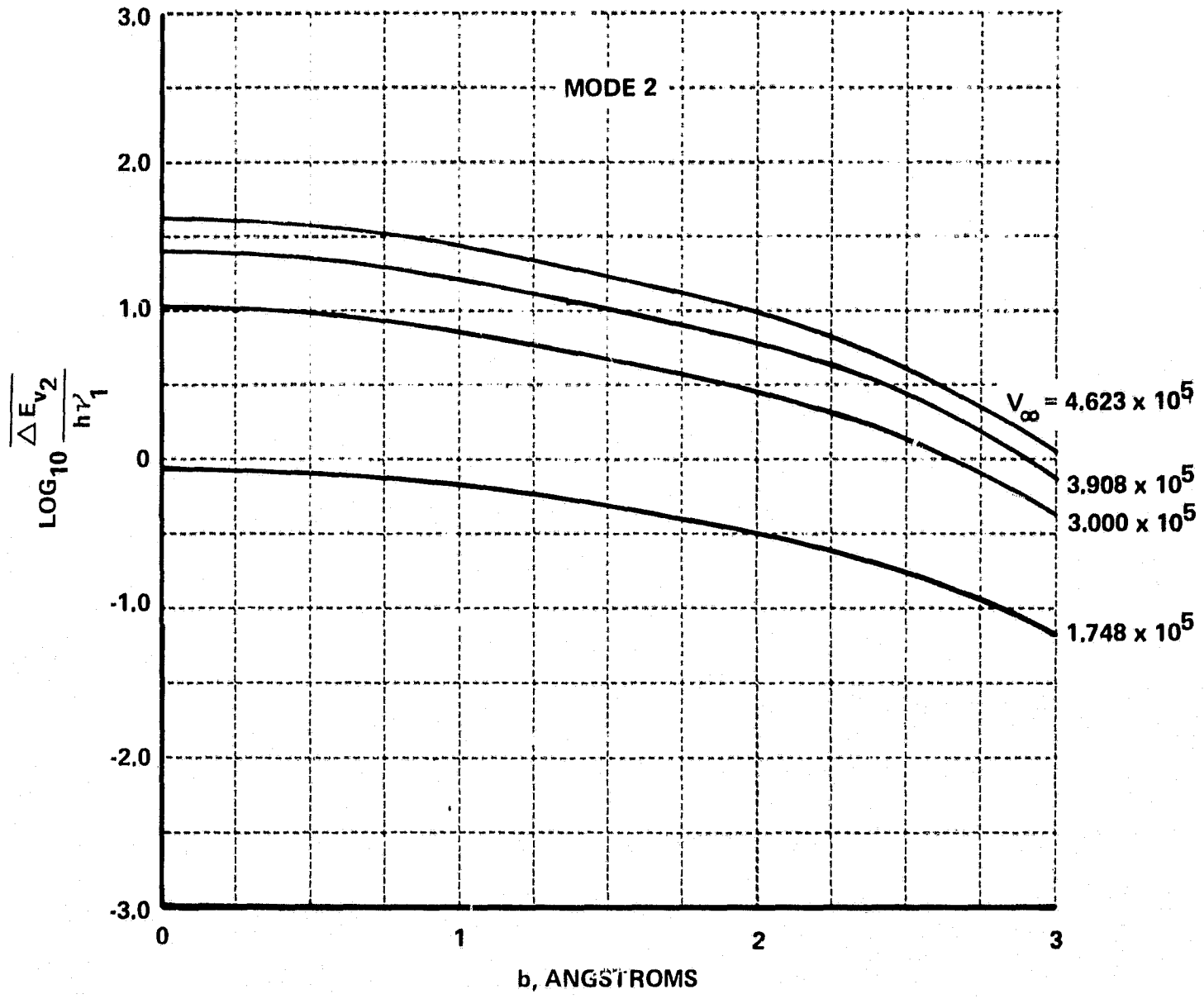

Figure 8 CLASSICAL ENERGY TRANSFERRED TO CO_2 ν_2 MODE IN COLLISION WITH Ar VS. IMPACT PARAMETER

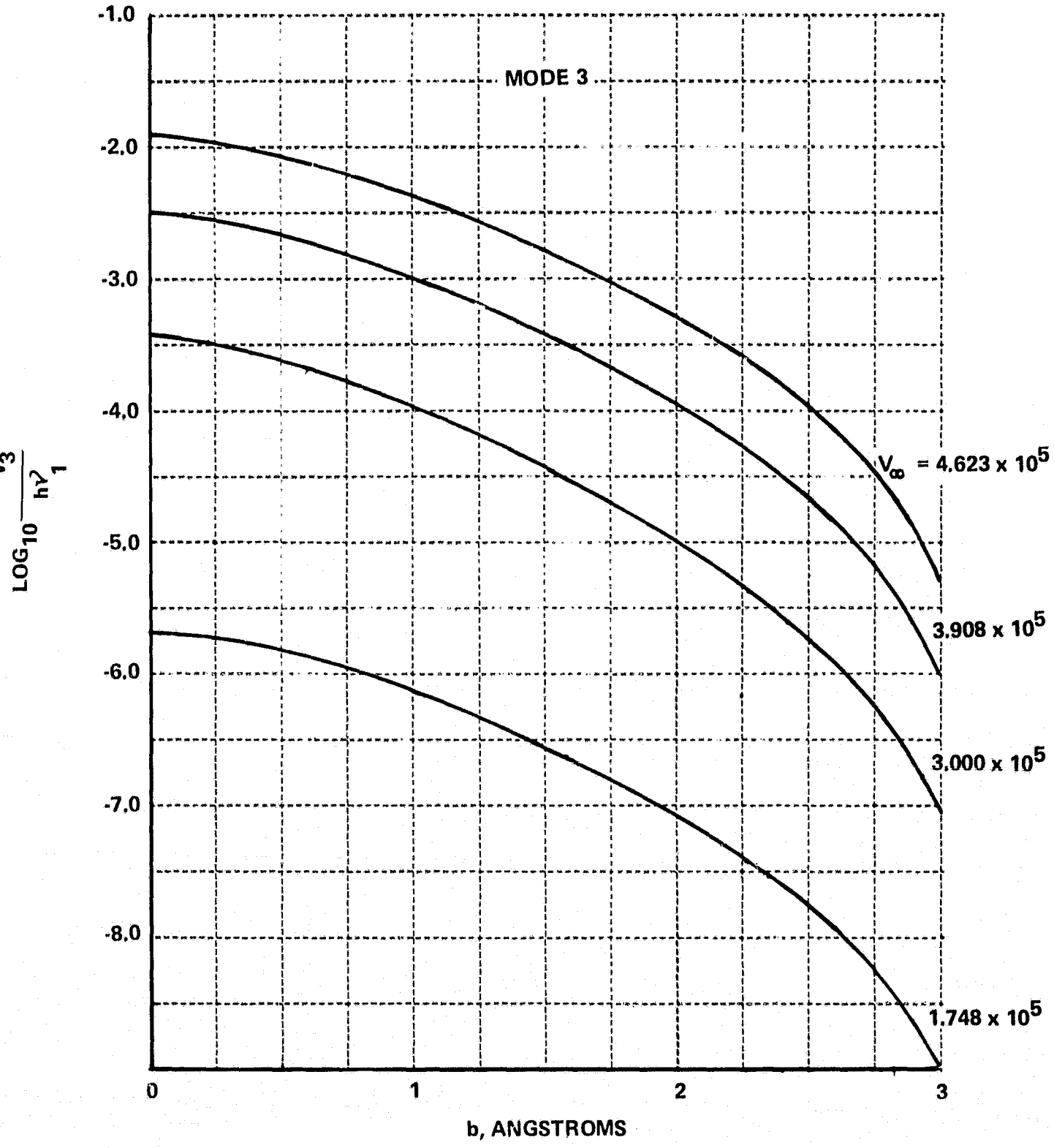

Figure 9 CLASSICAL ENERGY TRANSFERRED TO CO_2 ν_3 MODE IN COLLISION WITH Ar VS. IMPACT PARAMETER

of rapid intermode energy distribution, the CO_2 V-T relaxation is determined by the bending mode relaxation rate. The present formulation allows the bending mode excitation rate to be calculated independently of the other modes. This simplification will permit extensive examination of the influence of potential parameters on the predicted, thermally averaged V-T rate, and comparison of these rates with those experimentally measured. Generally, such parametric investigations would be difficult, since each predicted rate is obtained by incorporating many individual trajectory calculations into a thermal averaging scheme (Section 3). Parametric examination of the resulting rates generally would require a much larger amount of machine time if the influence of all modes had to be incorporated into every trajectory calculation.

A second advantage of the present model is that it permits straightforward calculation of the quantum mechanical transition probability, Eq (2-13). Quantum mechanical calculations for more complex models offer much greater difficulty (Section 6).

The limitations of this model analysis arise from four basic approximations:

1. Semiclassical Approximation
2. Normal Mode Approximation
3. Linearized Potential Approximation
4. Decoupling Approximation

The semiclassical approximation is invoked by treating both the rotational and translational motion of the system classically. The limitations imposed by this common assumption are discussed in standard references.[10] The approximation is unlikely to create any significant limitation for the present application.

The use of a normal mode approximation to the true CO_2 internal energy states does, of course, involve ignoring an important CO_2 feature: the close coupling among states in Fermi resonance. Further, terms coupling the rotational and vibrational motions, created by Coriolis and centrifugal forces, also are neglected. Finally, the normal mode approximation implies

small amplitude vibrational bending and stretching. The model given in this section obviously cannot shed any information on intramolecular energy transfer processes. This specific problem is addressed in Section 6 of this report. The present analysis, however, is directed toward calculation of the rate for the basic V-T vibrational excitation process. For this purpose, the normal mode approximation can provide useful information.

The last two approximations can be discussed together. Inaccuracies arising from use of the linearized potential and from the decoupling approximation can only be assessed in detail by performing a calculation in which these approximations are not made. A check of this nature involves numerical solution of the more general classical equations of motion for the CO_2-M system, with consequent loss of the computational advantages of the present model. Section 4 details such a general system of equations, in a form suitable for numerical integration. It is planned to perform this more exact calculation for a few check cases in order to establish definite limits on the validity of the decoupled calculation.

Pending the detailed comparison of the linearized, decoupled calculation with the exact classical calculation, some qualitative assessments of the limitations of the simpler model can be made. It is not expected that linearization of the potential in the vibrational displacements will affect the qualitative nature of the calculated ΔE_{v_i}'s or $P^i_{m\,n}$'s. The sensitivity of the cross sections to small changes in the intermolecular potential has, however, often been demonstrated for inelastic processes of this type. It must be assumed, therefore, that the inclusion of higher order potential terms may have an effect on the magnitude of the calculated cross sections, particularly at lower collision energies.

Turning to the effect of the decoupling approximation, 4, a definite consequence of this approximation can be seen in Figs. 4 and 5. The values of the rotational energy chosen for these curves bracket the energy range of interest. The $12.3\,h\nu_i$ run represents an extreme case. It should be noted that the ΔE_v curve for $(E_{ROT}/h\nu_i)_{\text{Initial}} = 12.3$, $i = 1$, shows a ΔE_v greater than the total available energy in collision at translational energies greater

than $\approx 10\, h\nu$. This violation of energy conservation reflects the fact that one of the model assumptions fails at extremely high energies. It will be recalled that the present semiclassical model assumes that the translational-rotational motion of the colliding molecules is not affected by molecular vibration. This decoupling approximation is not valid at extremely high energies, when the period of collisional interaction becomes smaller than the period of vibrational oscillation. Under such conditions, the vibrational motion is strongly coupled to the external (translational and rotational) motions of the molecules. The high energy failure is also evident in the bending mode ($i = 2$) curve, for $(E_{ROT} / h\nu)_{\text{Initial}} = 12.6$. It does not appear in the present runs for the ($i = 3$) curves, since the period of the asymmetric stretching mode is considerably shorter than the other CO_2 modes. This high energy limitation should not be of importance, however, even in the rather large energy range (0 to 1 ev) of current interest. Note that the model failure occurs when the total energy available in collision, $E_T + E_{ROT}$ approaches $20\, h\nu$. At the temperatures of interest, collisions with so large an available energy are rare.

3. MONTE CARLO CALCULATIONS

In the paragraphs below we will discuss the form of the integrals and the scheme to be used for the Monte Carlo thermal averaging of the $V-T$ transition probabilities developed in Section 2.

Using the coordinate system shown in Fig. 10, one can select a particular collision trajectory by specifying the initial position of the incoming structureless particle in spherical coordinates (R_o, Θ_o, Φ_o), the initial orientation of the CO_2 molecule (α_o, β_o), the initial rotational velocity $\vec{\omega}_o$ of the CO_2 molecule, and the initial relative velocity $\vec{V}_o$ between the molecules. Here the subscript zero has been used to indicate the initial values for the coordinates.

However, this coordinate system is completely arbitrary in orientation and is not the most convenient one to use for the quadrature. Consequently, we now choose a second coordinate system (dependent upon the parameters of the collision) such that the xy-plane is coincident with the plane determined by the line joining the centers of the two molecules (i.e. the direction specified by (R_o, Θ_o, Φ_o) above) and by the initial relative velocity $\vec{V}_o$. The orientation of this new coordinate system is completely specified if we choose the x-axis to be parallel, but oppositely directed to $\vec{V}_o$.

In this new coordinate system the incoming structureless particle appears as shown in Fig. 11. Now the initial parameters needed to specify the interaction are six in number: the magnitude of the incoming relative velocity V_o, the impact parameter b for the collision, the orientation (α_o, β_o) of the axis of the CO_2 molecule (now referred to the new coordinate system, but measured in the same fashion as shown in Fig. 10), and the angular velocity (ω_{α_o}, ω_{β_o}) of the CO_2 molecule. (Note that only two components are required to specify the angular velocity vector since this vector is orthogonal to the CO_2 molecular axis.)

One further alteration is needed to simplify the selection of the initial parameters for each collision trajectory. Rather than specify the initial angular velocity of the CO_2 molecule by the parameters ω_{α_o} and ω_{β_o}, we

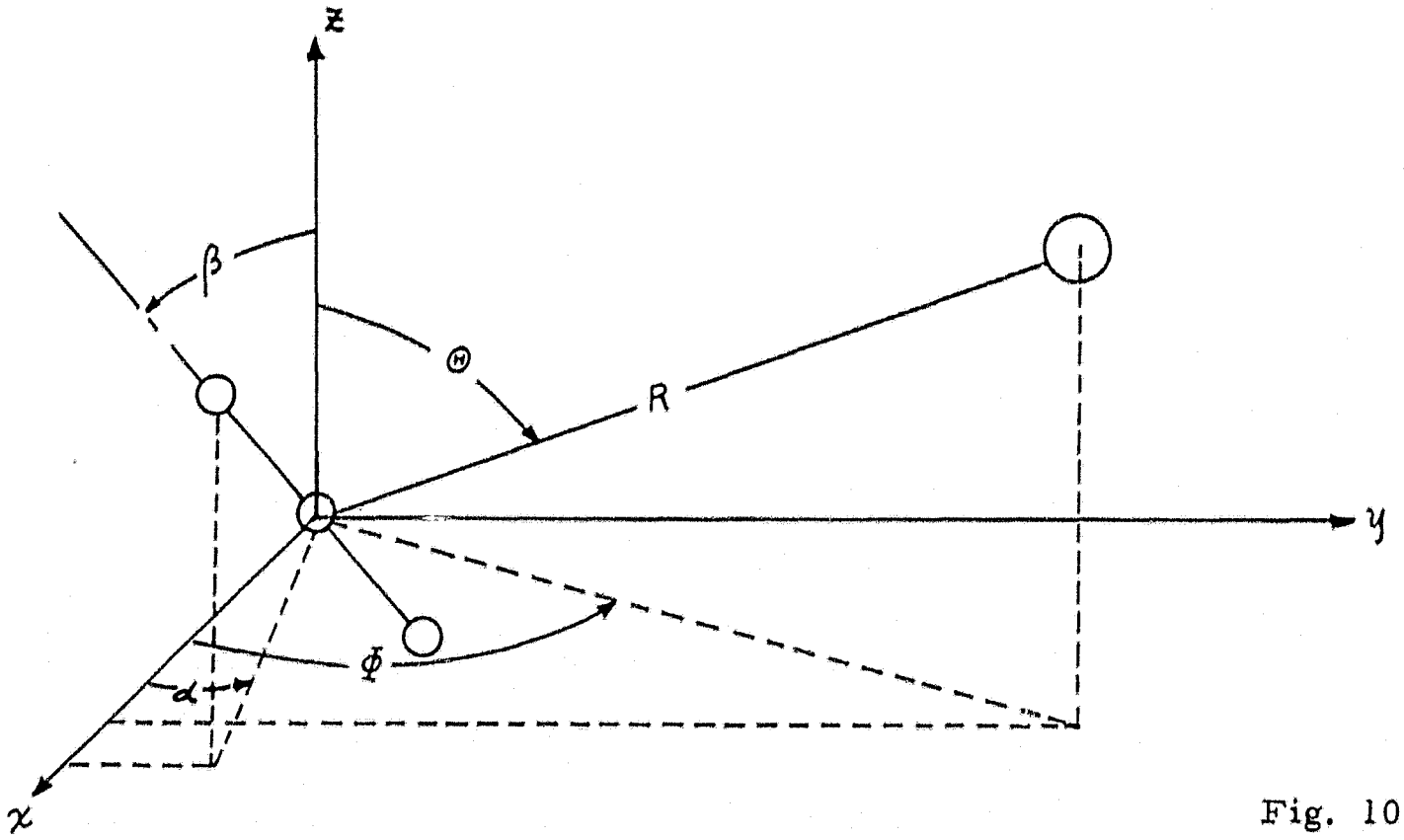

Fig. 10

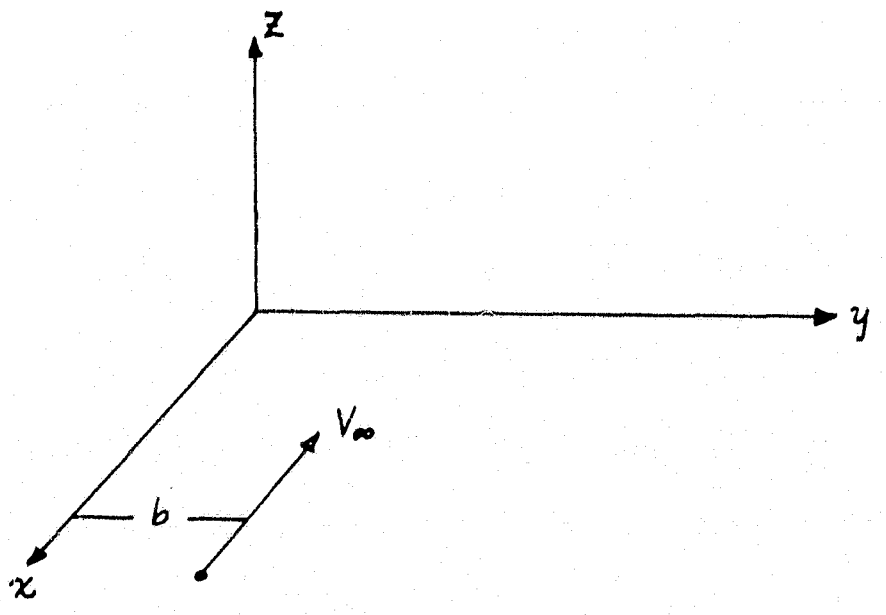

Fig. 11

choose the magnitude p of the angular momentum and an angle γ defining the direction of the angular momentum in phase space. ω_{α_o} and ω_{β_o} are found from p and γ as follows:

$$\omega_{\alpha_o} = \frac{1}{I}\, p \sin\gamma \sin\beta_o$$

$$\omega_{\beta_o} = \frac{1}{I}\, p \cos\gamma$$

The idea of the Monte Carlo calculation is to select "at random" the six initial parameters mentioned above for each of a large number of collisions, and from the computation of the corresponding trajectories to deduce the thermally-averaged energy transfer to the vibrational modes of the CO_2 molecule.

The Monte Carlo calculation of interest to us starts with integrals for the rate $R^i_{m\,n}$ of transition from the m^{th} vibrational level to the n^{th} vibrational level in the i^{th} mode (where i = 1, 2, 3 or 4). This rate depends upon the number density n_A of atoms, the number density n_{co_2} of CO_2 molecules and temperature T as well as upon the parameters α_j and c_j (j = 1, 2, 3) describing the interaction potential. If we denote by $P^i_{m\,n}(\epsilon_i)$ the probability for a transition in the i^{th} mode from state m to state n, then

$$P^i_{m\,n}(T) = n_A\, n_{co_2}\, 4\pi \left(\frac{M}{2\pi k T}\right)^{3/2} \int_o^\infty e^{-\frac{MV^2}{2kT}}\, V_o^3\, d\,V_o \int_o^{b*} 2\pi\, b\, d\, b$$

$$\frac{1}{(2\pi)^2\, I\, k\, T} \int_o^\pi \sin\beta_o\, d\,\beta_o \int_o^\pi d\,\alpha_o \int_o^{2\pi} d\,\gamma_o \int_o^\infty p\, d\, p\; e^{-p^2/2IkT}\, P^i_{m\,n}(\epsilon_i)$$

where b_* is a cut-off impact parameter

$$P^i_{m\,n}(\epsilon_i) = m!\, n!\, e^{-\epsilon_i}\, \epsilon_i^{\,m+n}\, S^2_{m\,n}$$

$$\epsilon_i = \Delta E_{v_i} / \hbar\,\omega_i$$

$$S_{m\,n} = \sum_{j=o}^{\mu} \frac{(-1)^j\, \epsilon_i^{-j}}{(n-j)!\, j!\, (m-j)!} \qquad \text{and} \qquad \mu = \min(m,n)$$

Dividing by the collision rate (the number of collisions per unit volume per unit time) $4\pi\, b_*^2\, n_A\, n_{co_2}\, (kT / 2\pi M)^{1/2}$, we obtain the probability of a transition from state m to state n in the i^{th} mode

$$P^{i}_{mn} = \frac{1}{2}\left(\frac{M}{kT}\right)^{2} \frac{1}{(2\pi)^{2} I k T} \int_{0}^{\infty} \exp\left[-\frac{M V_{o}^{2}}{2kT}\right] V_{o}^{3}\, d V_{o} \int_{0}^{b_{*}} 2\, \frac{b}{b_{*}}\, \frac{db}{b_{*}} \int_{0}^{\pi} \sin\beta_{o}\, d\beta_{o}$$

$$\int_{0}^{\pi} d\alpha_{o} \int_{0}^{2\pi} d\gamma \int_{0}^{\infty} p\, dp\, \exp\left[-p^{2}/2 I k T\right] P^{i}_{mn}(\epsilon_{i}) \qquad (3.1)$$

The central problem arising in any Monte Carlo calculation is the determination of a scheme or algorithm which will require a minimal time to calculate a reliable result. Such a scheme is termed efficient. The usual method for increasing the efficiency of a calculation is through the utilization of variance reducing techniques.[29,30] The variance is a measure of the accuracy of a particular scheme after a given number of trials. If one scheme is estimated to have a smaller variance than a second scheme, generally the former will be more efficient than the latter.

However, in the case of Eq (3.1) the efficiency of the calculation can be examined in a broader sense. The integral in Eq (3.1) depends upon the temperature, and evaluation of this integral is desired for many values of the temperature within the range $0 < T < 15000°K$. The integrals over α_{o}, β_{o}, γ and b do not involve temperature and can be performed by a straightforward application of the Monte Carlo technique. Examination of the integrals over V_{o} and p shows that the integrand is a product of two factors, the Boltzmann distribution involving T and the transition probability for a collision $P^{i}_{mn}(\epsilon_{i})$.

A trajectory calculation is required for each evaluation of the latter quantity, and these calculations are the most time-consuming aspect of the Monte Carlo computation. The integral, if evaluated by separate calculations for each of M values of the temperature, would require MN trajectory determinations, where N is the number of ordinates evaluated for each temperature. On the other hand, if the integral for $P^{i}_{mn}(T)$ could be evaluated for all M values of temperature for only one set of N trajectory calculations, a great saving in computational time could be achieved. At the highest end

of the temperature range, where the Boltzmann distributions are broad and not sharply peaked, this procedure should be very effective.

Mathematically, the device just described is carried out by utilizing the variance reducing technique called importance sampling. If the integrand is denoted by $f(\alpha_o, \beta_o, \gamma, b, V_o, p)$, the integral for P^i_{mn} can be written as

$$P^i_{mn}(T) = \int_o^{\pi} d\alpha_o \int_o^{\pi} d\beta_o \int_o^{2\pi} d\gamma \int_o^{b_*} db \int_o^{\infty} dV_o \int_o^{\infty} dp \; f(\alpha_o, \beta_o, \gamma, b, V_o, p)$$

We multiply and divide f by

$$g(\alpha_o, \beta_o, \gamma, b, V_o, p; \vartheta) = \frac{1}{2}\left(\frac{M}{k\vartheta}\right)^2 \exp\left[-\frac{MV_o^2}{2k\vartheta}\right] V_o^3 \left(2\frac{b}{b_*^2}\right)$$
$$\left(\frac{1}{2}\sin\beta_o\right) \frac{1}{2\pi^2} \frac{p}{I k\vartheta} \exp\left[-\frac{p^2}{2I k\vartheta}\right]$$

so that

$$P^i_{mn}(T) = \int_o^{\pi} d\alpha_o \int_o^{\pi} d\beta_o \int_o^{2\pi} d\gamma \int_o^{b_*} db \int_o^{\infty} dV_o \int_o^{\infty} dp \left[\frac{f}{g}\right] g .$$

The choice of the functional form of g with respect to V_o and p is dictated by heuristic considerations. If one were to examine a container filled with a mixture of CO_2 molecules and inert monatomic molecules, and if one labeled all random collisions between one of each type of molecule, the probability for energy transfer in a selection of N collisions would be simulated by an N-term Monte Carlo computation. The initial relative velocity V_o and angular momentum p of the CO_2 molecule would be chosen "at random" from a Boltzmann distribution for these quantities at the characteristic temperature ϑ of the mixture. Therefore, a Boltzmann-type probability density function g at a ficticious temperature ϑ would be an intuitive choice. Since the probability $P^i_{mn}(\epsilon_i)$ for energy transfer in any particular collision is small except for the most energetic collisions, the collisions with large initial values of V_o and p will contribute most to the energy transfer process. Therefore, the ficticious temperature ϑ is expected to be somewhat higher than the actual temperature T in the integral.

We introduce the convenient scale factors $V_{oo} = (k\vartheta/M)^{1/2}$ and

$p_{oo} = (I k v)^{1/2}$ together with the new integration variables $v = V_o/V_{oo}$ $q = p/p_{oo}$ and $b = b/b_*$. The expression for P^i_{mn} becomes

$$P^i_{mn}(T) = \int_o^{\pi} \frac{d\alpha_o}{\pi} \int_o^{\pi} \frac{d\beta_o}{\pi} \sin\beta_o \int_o^{2\pi} \frac{d\gamma}{2\pi} \int_o^{1} 2b\,db \int_o^{\infty} 1/2\, v^3\, dv\, \exp\left(-\frac{v^2}{2}\right)$$
$$\int_o^{\infty} q\, dq\, \exp\left(-\frac{q^2}{2}\right) \left\{\left(\frac{v}{T}\right)^3 \exp\left[-\frac{v}{2}(v^2+q^2)\left(\frac{1}{T}-\frac{1}{v}\right)\right] P^i_{mn}(\epsilon_i)\right\} \quad (3.2)$$

For the Monte Carlo estimate of this integral the probability density function is given by $g(\alpha_o, \beta_o, \gamma, b, v, q; v)$. A large number N of sets of values for α_o, β_o, γ, b, v and q are selected at random from this density function. Note that each set of values represents initial conditions for a trajectory and that each set is independent of the particular value chosen for T in the integral. Let the k^{th} set of values be denoted by $\alpha_o^{(k)}$, $\beta_o^{(k)}$, $\gamma^{(k)}$, $b^{(k)}$, $v^{(k)}$ and $q^{(k)}$, and

$$F^{(k)}(v, T; i, m, n) = \left(\frac{v}{T}\right)^3 \exp\left[-\frac{v}{2}(v^2+q^2)\left(\frac{1}{T}-\frac{1}{v}\right)\right] P^i_{mn}(\epsilon_i^{(k)}) \quad (3.3)$$

where $P^i_{mn}(\epsilon_i^{(k)})$ has been evaluated for the k^{th} set of values. The Monte Carlo approximation to $P^i_{mn}(T)$ is given by

$$P^i_{mn}(T) \cong \frac{1}{N} \sum_{k=1}^{N} F^{(k)}(v, T; i, m, n) \quad (3.4)$$

while the variance, an estimate of the magnitude of the error involved in the integral, is given by

$$\sigma^2 \cong \frac{1}{N} \sum_{k=1}^{N} \left[F^{(k)}(v, T; i, m, n)\right]^2 - \left[P^i_{mn}(T)\right]^2 \quad (3.5)$$

We reiterate that the single set of N trajectory calculations allows us to compute $P^i_{mn}(T)$ for several values of T . The initial values for each trajectory are selected at random from the probability density g , which is independent of T . The corresponding values of $P^i_{mn}(\epsilon_i^{(k)})$ are computed for each trajectory, these values also being independent of T . Finally, for any particular T the factors $F^{(k)}$ are calculated, using the $P^i_{mn}(\epsilon_i^{(k)})$, and these factors are summed to give the estimate of $P^i_{mn}(T)$.

For a range of temperatures this technique will be quite accurate. However, for temperatures beyond this range, the technique will begin to fail as a result of the lack of accuracy. Such loss will be evidenced by an increased σ^2 and also by a poorer convergence in $P^{i}_{mn}(T)$ as a function of the number N of trajectories.

We expect this procedure to yield accurate results over the widest temperature range for a given ϑ at the highest temperatures. At the lower temperatures a single value of ϑ will allow computation of the integral over a much smaller range of temperatures. However, in this range the functional form of $P^{i}_{mn}(\epsilon_i)$ obtained from the Monte Carlo computations at the higher temperatures will allow an optimal choice of ϑ for the temperature of interest.

4. FOUR-BODY CLASSICAL DESCRIPTION OF CO_2-M COLLISIONS

In this section, a completely classical four-body analysis for CO_2-M collisions is developed, without the decoupling approximation of Section 2.

4.1 HAMILTON'S EQUATIONS

Consider the four-body system of particles A, B, C, D with masses m_A, m_B, m_C, m_D, respectively. (For later specialization to CO_2-M collisions, A = M; B, D, = O; C = C). Let Q_j (j = 1, 2, 3) be the Cartesian coordinates of A with respect to the center of mass of BCD. Let Q_j (j = 4, 5, 6) be the Cartesian coordinate of B with respect to D. Let Q_j (j = 7, 8, 9) be the Cartesian coordinates of C with respect to the center of mass of BD. Finally, let Q_j (j = 10, 11, 12) be the Cartesian coordinates of the center of mass of the ABCD system.

The system Hamiltonian in terms of these coordinates and their conjugate momenta P_j is

$$H = \sum_{i=1}^{3} (2\mu_{A,M-A})^{-1} P_i^2 + (2\mu_{B,D})^{-1} P_{i+3}^2 + (2\mu_{C,B+D})^{-1} P_{i+6}^2$$

$$+ (2M)^{-1} P_{i+9}^2 + \vartheta (Q_1, Q_2, \ldots, Q_9) , \qquad (4\text{-}1)$$

where

$$\mu_{A,M-A} = \frac{m_A(m_B+m_C+m_D)}{M} , \quad \mu_{B,D} = \frac{m_B m_D}{m_B+m_D}$$

$$\mu_{C,B+D} = \frac{m_C(m_B+m_D)}{m_B+m_C+m_D} , \quad M = m_A + m_B + m_C + m_D$$

Note that in this coordinate system the Hamiltonian is diagonal in the kinetic energy, and the potential energy is only a function of Q_1, Q_2, ..., Q_9, so that the ABCD mass motion may be neglected.

The equations of motion are, accordingly:

$$\dot{Q}_i = \mu^{-1}_{A,M-A}\, P_i \qquad (4\text{-}2, 3, 4)$$

$$\dot{Q}_{i+3} = \mu^{-1}_{B,D}\, P_{i+3} \qquad (4\text{-}5, 6, 7)$$

$$\dot{Q}_{i+6} = \mu^{-1}_{C,B+D}\, P_{i+6} \qquad (4\text{-}8, 9, 10)$$

$$\dot{P}_i = -\frac{\partial \mathcal{V}}{\partial Q_i} \qquad (4\text{-}11, 12, 13)$$

$$\dot{P}_{i+3} = -\frac{\partial \mathcal{V}}{\partial Q_{i+3}} \qquad (4\text{-}14, 15, 16)$$

$$\dot{P}_{i+6} = -\frac{\partial \mathcal{V}}{\partial Q_{i+6}} \qquad (4\text{-}17, 18, 19)$$

$i = 1, 2, 3$ 18 equations in all.

4.2 POTENTIAL FUNCTIONS

The potential function $\mathcal{V}$ can be written as the sum of two parts, the intermolecular potential V_{INTER} and the intramolecular potential for the CO_2 molecule, V_{INTRA} . We discuss each of these in turn.

Intermolecular Potential Function

We take this potential to be a linear combination of four point-center interactions

$$V_{INTER}(r_i) = \sum_{i=1}^{4} f_i(r_i) \qquad (4\text{-}20)$$

r_i, $(i = 1, 2, 3)$ represents the distance from the incident particle to the i^{th} nucleus of the CO_2 molecule. r_4 is the distance between the center of mass of the molecule and the center of mass of the incident particle.

We have tentatively chosen, as in Section 2, for the f_i , simple exponential interactions. In particular, for the potentials centered on the nuclei, repulsive exponentials are used:

$$f_i = c_i e^{-\alpha_i r_i} \qquad i = 1, 2, 3 \qquad (4\text{-}21)$$

For the potential between the mass centers, an attractive exponential is used:

$$f_4 = - c_4 e^{-\alpha_4 r_4} \qquad (4\text{-}22)$$

The distances r_i can be written in terms of the generalized coordinates Q_j :

$$r_1 = \left\{ \sum_{j=1}^{3} \left[- Q_j + \left(\frac{m_B + m_D}{\mu} \right) Q_{j+6} \right]^2 \right\}^{1/2} \qquad (4\text{-}23)$$

$$r_2 = \left\{ \sum_{j=1}^{3} \left[- Q_j + \left(\frac{m_D}{m_B + m_D} \right) Q_{j+3} - \frac{m_c}{\mu} Q_{j+6} \right]^2 \right\}^{1/2} \qquad (4\text{-}24)$$

$$r_3 = \left\{ \sum_{j=1}^{3} \left[- Q_j - \left(\frac{m_B}{m_B + m_D} \right) Q_{j+3} - \frac{m_c}{\mu} Q_{j+6} \right]^2 \right\}^{1/2} \qquad (4\text{-}25)$$

$$r_4 = \left[\sum_{j=1}^{3} Q_j^2 \right]^{1/2} \qquad (4\text{-}26)$$

for $j = 1, 2, 3$

Intramolecular Potential Function

In the classical model discussed in this section, attention is confined to harmonic vibrational potentials in the CO_2 molecule. (A model to examine the effects of anharmonicity in CO_2-M collisions is discussed in Section 6.) If S_1 , S_2 , S_3 are the dimensional displacements in the normal mode directions for CO_2 (see Appendix B) we have:

$$V_{INTRA} = + \frac{1}{2} \sum_{i=1}^{3} C_{ii} S_i^2 , \qquad (4\text{-}27)$$

where

$$S_1 = \left| \bar{Q}_{j+3} \right| - 2\ell \qquad (4\text{-}28)$$

$$S_2 = \left| \bar{Q}_{j+6} \times \bar{Q}_{j+3} \right| \Big/ \left| \bar{Q}_{j+3} \right| \qquad (4\text{-}29)$$

$$S_3 = \bar{Q}_{j+6} \cdot \bar{Q}_{j+3} \Big/ \left| \bar{Q}_{j+3} \right| \qquad (4\text{-}30)$$

and

$$\bar{Q}_{j+n} = Q_{1+n} \hat{i} + Q_{2+n} \hat{j} + Q_{3+n} \hat{k}$$

ℓ = equilibrium C-O separation

To obtain the derivatives of the potential with respect to the Q_i used in the equations of motion (4-11 - 4-19), we use the chain rule:

$$\frac{\partial \vartheta}{\partial Q_j} = \sum_K \left(\frac{\partial \vartheta}{\partial r_K} \frac{\partial r_K}{\partial Q_j} + \frac{\partial \vartheta}{\partial S_K} \frac{\partial S_K}{\partial Q_j} \right) \qquad (4\text{-}31)$$

Initial Conditions

We require the specification of nine Q_j's and nine P_j's. To specify these, we take the initial orientation of the molecule and incident atom as follows:

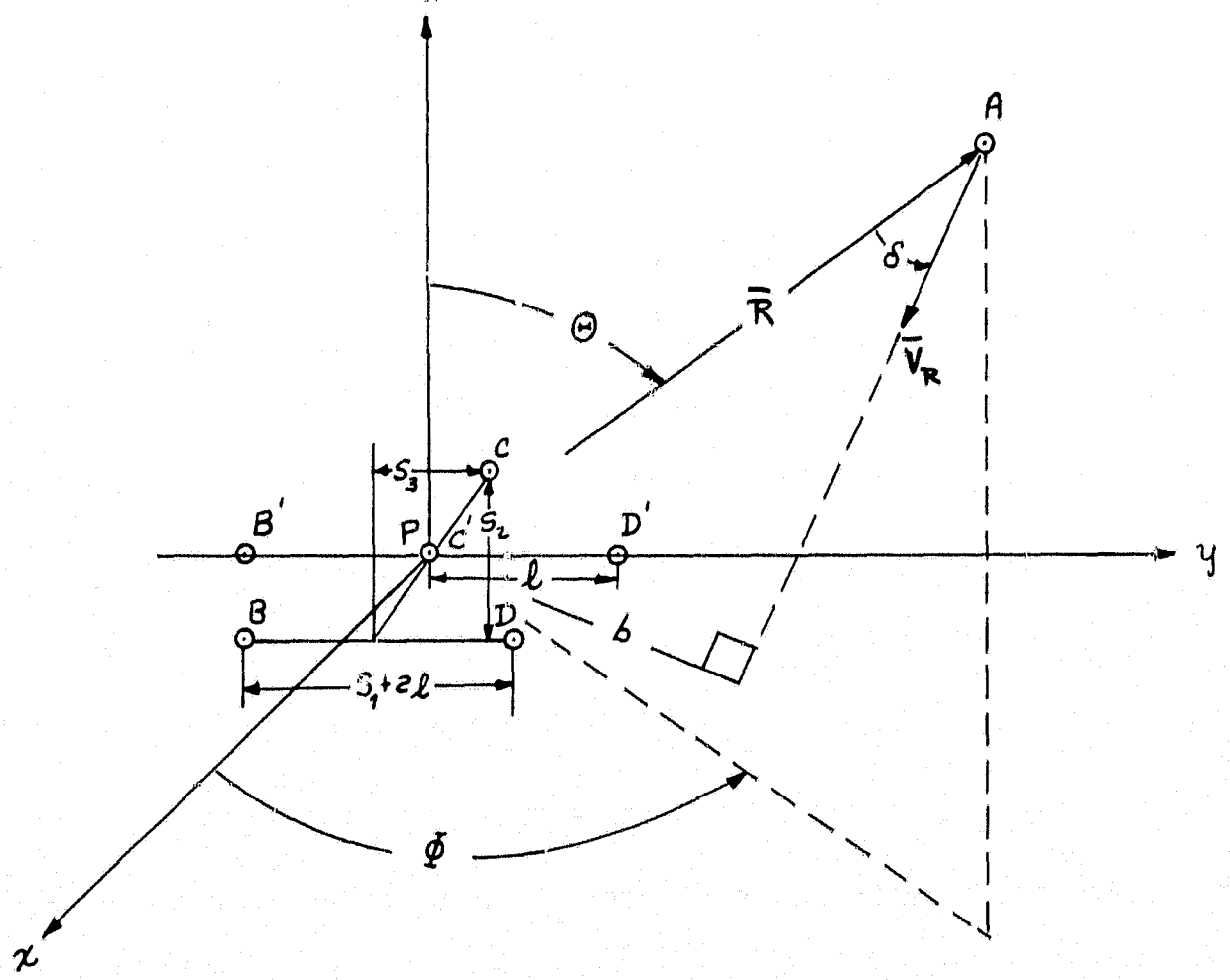

Figure 12

The xyz system is so chosen that its origin is at the center of mass of the molecule (point P) and the zy plane is the plane of bending. The equilibrium molecular axis lies along P-y . B'C'D' are the equilibrium (non-vibrating) positions of the nuclei in the molecule. B-C-D are the actual initial positions of the nuclei, after they have been given some vibrational displacement (arbitrary, except that P-y must be the molecular axis, P must be the C. M. location, and B'C'D' must remain in the zy plane).

Incident Atom

P_j , Q_j , $j = 1, 2, 3$, are the generalized coordinates of the incident atom, whose initial value specification we shall discuss first.

From the figure, we see

$$Q_1 = R \sin\Theta \cos\Phi \tag{4-32}$$

$$Q_2 = R \sin\Theta \sin\Phi \tag{4-33}$$

$$Q_3 = R \cos\Theta \tag{4-34}$$

Thus, $Q_{1,2,3}$ requires specification of R_o , Θ_o , Φ_o . It can also be shown that:

$$P_1 = \mu_{A,M-A} V_R \left(\cos\Phi \cos\Theta \sin\delta \cos\chi - \sin\Phi \sin\delta \sin\chi - \cos\Phi \sin\Theta \cos\delta\right)$$

$$P_2 = \mu_{A,M-A} V_R \left(\sin\Phi \cos\Theta \sin\delta \cos\chi + \cos\Phi \sin\delta \sin\chi - \sin\Phi \sin\Theta \cos\delta\right)$$

$$P_3 = \mu_{A,M-A} V_R \left(-\sin\Theta \sin\delta \cos\chi - \cos\Theta \cos\delta\right) ,$$

where $\delta = \sin^{-1} b/R_o$, b being the impact parameter. χ is the angle between the $\bar{V}_R - \bar{R}$ and the $\bar{z} - \bar{R}$ planes. Thus $P_{1,2,3}$ requires the specification of V_R , χ , and b in addition to R_o , Θ_o , Φ_o .

Molecule

P_j , Q_j , for $j = 4, 5, \ldots 9$, describe the molecule. Figure 3 shows the vibrational displacements in the normal coordinate directions, S_1 , S_2 , S_3 :

$S_1 + 2\ell$ is the displacement of the two O atoms relative to each other (2ℓ is the equilibrium displacement).

S_2 is the displacement of the C atom $\perp$ to the figure axis (i. e., y axis) relative to the line joining the O atoms.

S_3 is the displacement of the C atom along the figure axis relative to the c. m. of the O atoms.

We have initially:

$$Q_4 = 0$$

$$Q_5 = S_1 + 2\ell$$

$$Q_6 = 0 \qquad (4\text{-}38, \ldots, \text{-}43)$$

$$Q_7 = 0$$

$$Q_8 = S_3$$

$$Q_9 = S_2$$

Thus, $Q_{4,5\ldots9}$ requires the specification of initial values for the normal displacements S_1 , S_2 , S_3 .

There remains the specification of the conjugate momenta P_4 , $P_5 \ldots P_9$. If q_4 , q_5 , q_6 are the Cartesian coordinates of B,

q_7 , q_8 , q_9 are the Cartesian coordinates of C, and q_{10} , q_{11} , q_{12} are the Cartesian coordinates of D, it can be shown that:

$$P_{i+3} = \mu_{B,D} \left(\dot{q}_{i+3} - \dot{q}_{i+9} \right)$$

$$P_{i+6} = \mu_{C,B+D} \dot{q}_{i+6} + \frac{m_B m_C}{\mu} \dot{q}_{i+3} - \frac{m_C m_D}{\mu} \dot{q}_{i+9} \qquad i = 1, 2, 3$$

Thus, the problem of specifying P_4 , $P_5 \ldots P_9$ becomes a problem of specifying $\dot{\bar{q}}_{i+3} = \dot{q}_4 \hat{\imath} + q_5 \hat{\jmath} + \dot{q}_6 \hat{k}$, $\dot{\bar{q}}_{i+6}$ and $\dot{\bar{q}}_{i+9}$; i. e., the velocities of particles B , C , D in the molecule. If $\bar{\omega}$ is the rotational velocity of the molecule, and $\dot{\bar{\xi}}_{i+3}$, $\dot{\bar{\xi}}_{i+6}$, $\dot{\bar{\xi}}_{i+9}$ are the velocities (due to vibration) of B , C , D with respect to the rotating molecular axis,

$$\dot{\bar{q}}_{i+3} = \dot{\bar{\xi}}_{i+3} + \bar{\omega} \times \bar{r}_B$$

$$\dot{\bar{q}}_{i+6} = \dot{\bar{\xi}}_{i+6} + \bar{\omega} \times \bar{r}_C$$

$$\dot{\bar{q}}_{i+9} = \dot{\bar{\xi}}_{i+9} + \bar{\omega} \times \bar{r}_D \ ,$$

where $\bar{r}_B$, $\bar{r}_C$, $\bar{r}_D$ are the position vectors of B , C , D with respect to the origin.

If σ , ϵ are respectively the polar and azimuthal angular coordinates of $\bar{\omega}$, it can be shown that the initial values of P_4 , $P_5 \ldots P_9$ are given by:

$$P_4 = \frac{m_B m_D}{m_B + m_D} \left\{ \cos\sigma\ \omega (S_1 + 2\ell) + \frac{2 m_C}{m_B + m_C + m_D} \sin\sigma \sin\epsilon\ \omega S_2 \right\}$$

$$P_5 = \frac{m_B m_D}{m_B + m_D} \dot{S}_1$$

$$P_6 = \frac{-m_B m_D}{m_B + m_D} \sin\sigma \cos\epsilon\ \omega (S_1 + 2\ell)$$

$$P_7 = \frac{m_C (m_B + m_D)}{m_B + m_C + m_D} \left\{ \frac{m_B + m_D}{m_B + m_C + m_D} \sin\sigma \sin\epsilon\ \omega S_2 - \cos\sigma\ \omega S_3 \right\}$$

$$P_8 = \frac{m_C (m_B + m_D)}{m_B + m_C + m_D} \left\{ \dot{S}_3 - \sin\sigma \cos\epsilon\ \omega S_2 \right\}$$

$$P_9 = \frac{m_C (m_B + m_D)}{m_B + m_C + m_D} \left\{ \dot{S}_2 + \frac{m_B + m_D}{m_B + m_C + m_D} \sin\sigma \cos\epsilon\ \omega S_2 + \frac{m_C}{m_B + m_C + m_D} \omega S_3 \right\}$$

Finally, for the initial orientation of Fig. 12,

$$\omega = \left[\omega_\alpha^2 + \omega_\beta^2 + \omega_\gamma^2 \right]^{1/2}$$

$$\cos\sigma = \omega_\alpha / \omega$$

$$\cos\epsilon = \omega_\beta / \omega,$$

where ω_α is the initial molecular rotational velocity about the z axis,
ω_β is the initial molecular rotational velocity about the x axis, and
ω_γ is the angular velocity (initially about the y axis) associated with rotation of the bending plane of the CO_2 molecule.

5. ANALYTICAL STUDIES

5.1 MODELING OF THE EFFECT OF POTENTIAL ANISOTROPY AND MOLECULAR ROTATION

The models for CO_2-M molecular collisions developed in this report have retained the effect of molecular rotation; the intermolecular potential function is not sp. rically symmetric, and the CO_2 molecule is allowed to rotate during the collision. The equations of motion for such a system are much more complex than those for the more commonly adopted colinear or spherically symmetric models. As discussed in the preceding sections, anything approaching an exact solution of these equations can only be achieved by numerical integration. It is desirable, however, to have some analytic means of examining the effect of molecular rotation on the vibrational relaxation process, if only to give the qualitative dependence of the cross sections on rotational velocity. This section presents an analysis of a greatly simplified model that provides such a guide to rotational effects.

The analysis is confined to the symmetric stretching mode of linear molecules. For specivity, we consider the CO_2 symmetric stretching mode, using the notation of Section 2. The results will be applicable to any linear triatomic or diatomic molecule.

The model analyzed here is a further approximation to the model assumptions of the decoupled, normal-mode study of CO_2-M collisions given in Section 2. In that section, it was shown that if the effect of vibrational motion on the classical trajectory for the collision was neglected, and if the intermolecular potential was linearized in the vibrational displacements, the classical energy transferred to the symmetric stretching mode during collision is given by:

$$\Delta E_v = \frac{1}{2\mu}\left|\int_{-\infty}^{\infty} f(t)\, e^{i\omega_v t}\, dt\right|^2 = \frac{1}{2\mu}\,|J|^2, \tag{5-1}$$

where ω_v is the radial vibrational frequency for the symmetric stretching mode, and μ is the reduced mass for vibration of that mode. The effect of

the collision is represented in $f(t)$, the (linear) forcing function for the symmetric stretching mode. This is given by Eq (2-7a) of Section 2 as:

$$f = -2C_2\alpha_2 e^{-\alpha_2 R}\left[\frac{l}{R}\cos h(\alpha_2 l\cos\Theta') + \cos\Theta'\sin h(\alpha_2 l\cos\Theta')\right] \tag{5-2}$$

Following Parker,[23] the hyperbolic functions are expanded in a Fourier series. The Fourier coefficients are found to be the integral representations for Bessel functions of imaginary argument :

$$\cos h(\alpha_2 l\cos\Theta') = \sum_{-\infty}^{\infty} I_{2n}(\alpha_2 l)\, e^{2ni\Theta'} \tag{5-3}$$

$$\sin h(\alpha_2 l\cos\Theta') = \sum_{-\infty}^{\infty} I_{2n+1}(\alpha_2 l)\, e^{(2n+1)i\Theta'} \tag{5-4}$$

These are expansions in terms of a potential anisotropy parameter, $\alpha_2 l \equiv l/L$, the ratio of the anisotropy l to the potential range L. The coefficients decrease with increasing order, falling off more rapidly with decreasing $\alpha_2 l$.

Substituting (5-2), (5-3), and (5-4) into (5-1) gives

$$J = -2C_2\alpha_2\sum_{-\infty}^{\infty} S_n, \tag{5-5}$$

where

$$S_n = \int_{-\infty}^{\infty} A_n(t)\, e^{j(\omega_v t + 2n\Theta')}\, dt, \tag{5-6}$$

$$A_n = e^{-\alpha_2 R}\left[\frac{l}{R} I_{2n} + \frac{1}{2}\left(I_{2n+1} + I_{2n-1}\right)\right] \tag{5-7}$$

To this point, the analysis has been formal and remains general. Equations (5-5) - (5-7), however, do display explicitly the sensitive dependence of rotational effects on the anisotropy parameter l/L. It is seen that the effect of molecular rotation (which enters the expression principally through the $\Theta'(t)$ parameter) will be considerable for those cases in which the higher harmonics in Eq (5-5) have significant amplitudes, i.e., for cases $l/L > 1$.

To make further analytical progress, mathematically tractable approximate forms for $A_n(t)$ and $\Theta'(t)$ must be obtained allowing integration of S_n. We proceed to enumerate physical approximations which lead to a tractable model.

We assume:

1. Coplanar interactions, with all motion in the atom-molecule plane.
2. No translation-rotation coupling. This leads to the molecule possessing constant rotational velocity during the collision, and enables $R(t)$ to be calculated on the basis of a spherically symmetric interaction.
3. The classical form of the "modified wave number" (MWN) approximation will be introduced.

Some discussion of these approximations is necessary. The first assumption will hardly change the nature of the phenomena being investigated, as most features are retained in coplanar interactions. (We also note that the available classical machine solutions[4, 15] for vibrational excitation of a rotating diatomic are confined to the coplanar case, and therefore direct comparison of the present approximate theory and these exact numerical solutions will be possible.)

The second assumption is supported by the detailed machine calculations of Cross and Herschbach[31] for rigid rotator-atom collisions. They find that the deviation in the translational trajectory created by physically reasonable potential anisotropies is generally small. More importantly, for cases in which the molecular angular momentum is large compared with the orbital angular momentum, the effect of changes in rotational energy is small. Since we are most interested in the effects of large rotational velocities, the approximation is appropriate. In general, the approximation is poorest for high-impact-parameter, high-energy collisions. These are also the trajectories for which the MWN approximation (see below) is poorest. However, large impact-parameter collisions are the least important for effecting vibrational transition.[8]

The MWN approximation enables non-zero impact parameter collisions to be treated. First developed by Takayanagi for quantum mechanical treatments of vibrational excitation, its classical analog has been used by Nikitin.[32] Detailed comparison by Takayanagi[33] with calculations made by Salkoff and Bauer[33] without this approximation show that it is good at least to energies of a few eV. The nature of this approximation is best shown by discussing the trajectory equations:

Using the coordinate system of Fig. 10, if we confine the interaction to the xy plane, $\Theta = \beta = \pi/2$. Invoking approximation (2), the collision trajectory is governed by the equations of motion

$$M(\ddot{R} - R\dot{\Phi}^2) = -\frac{d\,V(R)}{d\,R} \tag{5-8}$$

and

$$R^2\dot{\Phi} = R_o^2\dot{\Phi}_o = V_\infty b \tag{5-9}$$

where R_o and $\dot{\Phi}_o$ are the values of R and $\dot{\Phi}$ at the classical turning point, and the other notation is the same as that of Section 2. From these equations, the well-known integral of motion for the time-distance relationship is obtained:

$$t = \int_{R_o}^{R}\left[V_\infty^2\,(1 - b^2/R^2) - \frac{2}{M}\,V(R)\right]^{-1/2} d\,R\,, \tag{5-10}$$

where $t = 0$ at $R = R_o$.

The basis of the MWN approximation is to replace the centrifugal term b^2/R^2 in (5-10) with its value at the classical turning point, b^2/R_o^2. This substitution is justified by the fact that the maximum contribution to the perturbation integral J in (5-1) comes from the region near the turning point. Finally, in the same spirit as this approximation, we replace $\dot{\Phi} = (R_o/R)^2\dot{\Phi}_o$ by its value at the turning point, $\dot{\Phi} \approx \dot{\Phi}_o$, and replace the (small) $(l/R)I_{2n}$ term in Eq (5-7) by $(l/R_o)I_{2n}$.

With these approximations, Eq (3-12) can be integrated for $V(R)$ given by (2-5a) with $\alpha_4 = \frac{1}{2}\alpha_1$, $\alpha_1 = \alpha_2$, to yield

$$e^{-\alpha_2 R} = \left[K_1 \cosh\left(\frac{\alpha_1 \bar{V}_\infty}{2} t\right) - K_2 \right]^{-2}, \tag{5-11}$$

where

$$K_1 \equiv \frac{(2 M \bar{V}_\infty^2 C_1 + C_4^2)^{1/2}}{M \bar{V}_\infty^2}, \qquad K_2 \equiv \frac{C_4}{M \bar{V}_\infty^2} \tag{5-12}$$

$$\bar{V}_\infty^2 \equiv V_\infty^2 \left(1 - b^2/R_o^2\right) \tag{5-13}$$

Using (5-11) and $\Theta' = \alpha - \Phi \approx (\omega_R - \dot{\Phi}_o) t + \eta$, where ω_R is the rotational velocity of the molecule and η is an arbitrary phase angle, Eq (5-6) becomes:

$$S_n = a_n e^{2ni\eta} \int_{-\infty}^{\infty} \frac{e^{i\omega n t} \, dt}{\left[K_1 \cosh\left(\frac{\alpha_1}{2} \bar{V}_\infty t\right) - K_2\right]^2} \tag{5-14}$$

where

$$a_n = \left[\frac{\ell}{R_o} I_n + \frac{1}{2} (I_{2n+1} + I_{2n-1}) \right]$$

$$\omega_n = \omega_v + 2n (\omega_R - \dot{\Phi}_o)$$

Eq (5-14) can be integrated by contour integration, yielding

$$S_n = \frac{4\pi a_n e^{2ni\eta}}{\alpha_1 \bar{V}_\infty^2 (K_1^2 - K_2^2)} \operatorname{cosech} \frac{2\pi\omega_n}{\alpha_1 \bar{V}_\infty} \left\{ \cot\phi \cosh\left[\frac{2\omega_n}{\alpha_1 \bar{V}_\infty} (\pi - \phi)\right] + \frac{2\omega_n}{\alpha_1 \bar{V}_\infty} \sinh\left[\frac{2\omega_n}{\alpha_1 \bar{V}_\infty} (\pi - \phi)\right] \right\} \tag{5-15}$$

where

$$\phi = \cos^{-1}(K_2 / K_1)$$

Using Eq (5-1), we have for the classical amount of energy transferred to the vibrational mode, when averaged over the phase η :

$$\Delta E_v = \frac{1}{4\pi\mu} \int_0^{2\pi} |J|^2 \, d\eta$$

$$= \frac{C_1^2 \alpha_1^2}{\pi\mu} \int_0^{2\pi} \left| \sum_{-\infty}^{\infty} S_n \right|^2 d\eta \tag{5-16}$$

Using (5-15), and integrating over phase* reduces this expression to the sum of square terms:

$$\Delta E_v = \frac{4\pi C_1^2}{\mu \bar{V}_\infty^2 (K_1^2 - K_2^2)} \sum_{n=-\infty}^{n=\infty} \left[\frac{\ell}{R_0} I_{2n} + \frac{1}{2}(I_{2n+1} + I_{2n-1}) \right]^2 . \qquad (5\text{-}17)$$

$$\operatorname{cosec} h^2 \left(\frac{2\pi\omega_n}{\alpha_1 \bar{V}_\infty} \right) \left\{ \cot\phi \cos h \left[\frac{2\omega_n}{\alpha_1 \bar{V}_\infty} (\pi - \phi) \right] + \frac{2\omega_n}{\alpha_1 \bar{V}_\infty} \sin h \left[\frac{2\omega_n}{\alpha_1 \bar{V}_\infty} (\pi - \phi) \right] \right\}^2 .$$

An especially simple case of Eq (5-17) occurs at higher collision energies, when the influence of the attractive part of the potential is negligible. At the higher energies, $M V^2 \gg C_4$, so that $K_2 = C_4 / M V^2$. Note that $C_4 = O(10^{-3} C_1)$ so that $K_1 \gg K_2$ at high energies, and $\phi \to \frac{\pi}{2}$. For this case, Eq (5-17) reduces to:

$$\Delta E_v = \frac{4\pi M^2}{\mu \alpha_1^2} \sum_{n=-\infty}^{\infty} \left[\frac{\ell}{R_0} I_2 + \frac{1}{2}(I_{2n+1} + I_{2n-1}) \right]^2 \omega_n^2 \operatorname{cosec} h^2 \left(\frac{2\pi\omega_n}{\alpha_1 \bar{V}_\infty} \right) \sin h^2 \left(\frac{\pi\omega_n}{\alpha_1 \bar{V}_\infty} \right) . \qquad (5\text{-}18)$$

Figures 13 and 14 are plots of $\ln \frac{\Delta E_v}{h\nu}$ vs nondimensionalized translational energy, $\frac{E_T}{h\nu}$, where $E_T = \frac{1}{2} M V_\infty^2$. These calculations were performed for zero impact parameter, $b = 0$ cases. The vibrational parameters are those of the symmetric stretching mode of CO_2 . (The potential parameters are values for CO_2 - Ar collisions, taken by matching the Morse potential of Eq (2-5a) to the Lennard-Jones viscosity parameters tabulated in Ref 28.) In Fig. 13, the repulsive potential centers have been taken to be at a distance (ℓ) of half the equilibrium C-O separation in the CO_2 molecule. In Fig. 14, ℓ is equal to the equilibrium C-O separation. The three curves shown in each figure are for various amounts of molecular rotational energy $E_R / h\nu$ where $E_R = \frac{1}{2} I \omega_R^2$.

The large difference in magnitude between Fig. 13 and Fig. 14 illustrates

---

* It is a consequence of the decoupling approximation (2), that enables immediate integration over rotational phase. The same feature occurs with respect to vibrational phase in obtaining Eq (5-1).

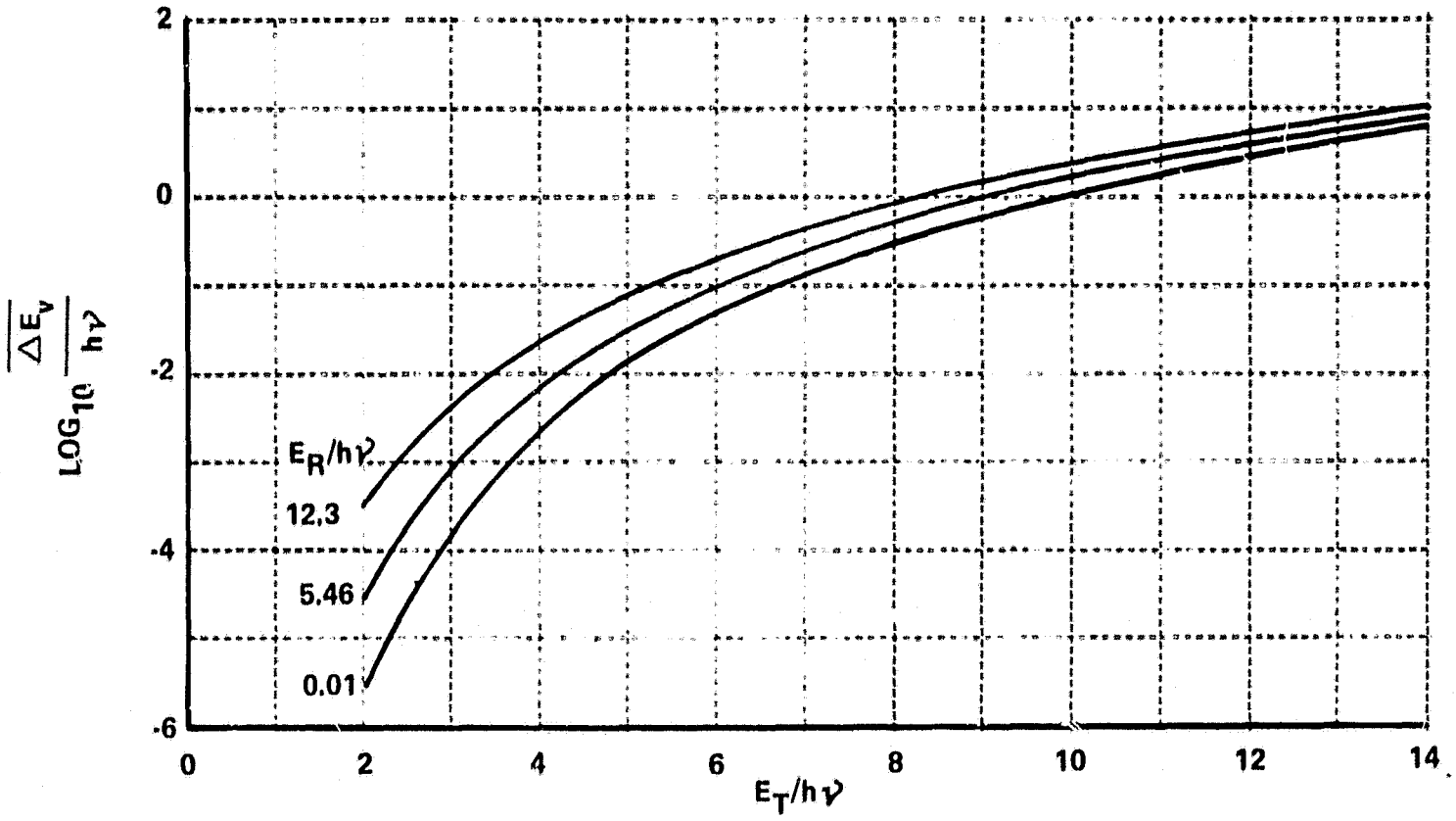

Figure 13 CLASSICAL ENERGY ΔE_v TRANSFERRED TO SYMMETRIC STRETCHING MODE OF CO_2 DURING COLLISION WITH Ar, AS A FUNCTION OF COLLISION ENERGY. PLOTS FOR VARYING AMOUNTS OF CO_2 ROTATIONAL ENERGY, $\alpha_2 \ell$ = 2.2 - APPROXIMATE ANALYTICAL MODEL (SEC. 5)

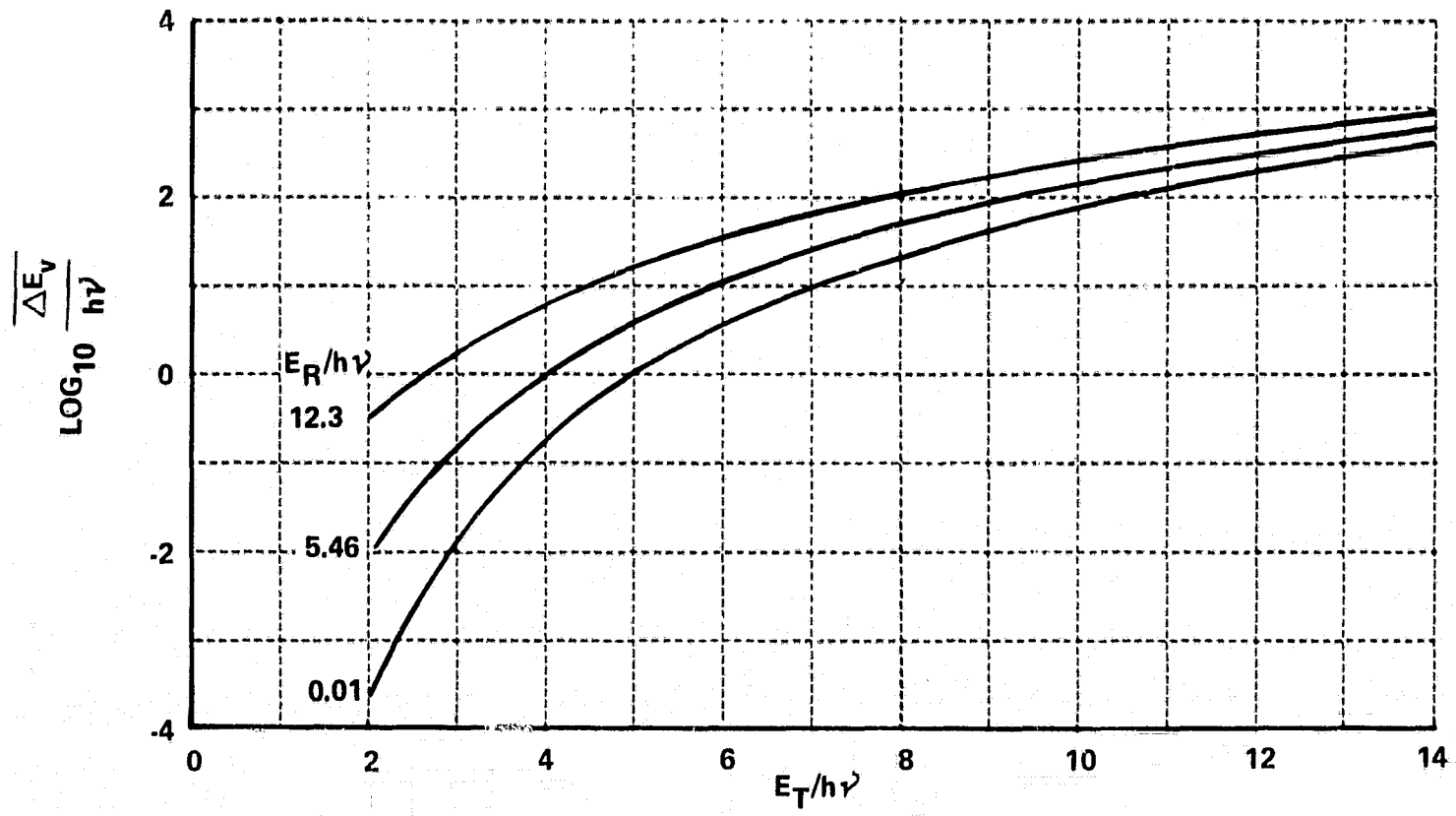

Figure 14 CLASSICAL ENERGY ΔE_v TRANSFERRED TO SYMMETRIC STRETCHING MODE OF CO_2 DURING COLLISION WITH Ar, AS A FUNCTION OF COLLISION ENERGY. PLOTS FOR VARYING AMOUNTS OF CO_2 ROTATIONAL ENERGY, $\alpha_2 \ell$ = 4.4 - APPROXIMATE ANALYTICAL MODEL (SEC. 5)

the sensitivity of the calculated ΔE_v's to the degree of potential anisotropy, i.e., to the ratio $\alpha_2 \ell * \ell / L$. As mentioned previously, this dependence on the potential anisotropy is evident in the original expansion, Eqs (5-5) - (5-7). The approximate analytic formula for ΔE_v , Eq (5-18), however, displays these features more explicitly.

Examining the sum in Eq (5-18) shows two effects of increasing the ratio $\alpha_2 \ell * \ell / L$;

i) The influence of molecular rotation is increased, inasmuch as the higher order terms in Eq (5-18) contribute more significantly to the sum, the ratios of the coefficients a_n not decreasing so rapidly with n .

ii) The actual magnitude of ΔE_v is critically dependent on $\alpha_2 \ell$ since the coefficients a_n increase rapidly with increasing $\alpha_2 \ell$.

Correlation of recent calculations[35, 36] of rotational relaxation times (using machine computation of coplanar rigid-rotator collisions) with experimental data suggests placement of the repulsive centers at approximately half the equilibrium nuclear separation. An accurate value is, however, quite an open question. The anisotropy constant must be regarded in the same light as the other parameters α_1 , α_4 , C_1 , C_4 in the model potential.

Figures 13 and 14 also illustrate the effect of molecular rotation. For those values of $E_T < E_R$, there is a considerable increase in ΔE_V for the rotating case, compared to the nonrotating case. For a given E_T , this enhancement increases with E_R . Above $E_T \approx E_R$ the enhancement due to rotation is not as marked; it appears that the rotational and translational energies are approximately equal in their contribution to ΔE_v .

Figures 15 and 16 show ΔE_v calculated for zero impact parameter and for molecular parameters characteristic of O_2 - Ar collisions, using Eq (5-18). (For these curves, the repulsive potentials have been centered on the equilibrium nuclear positions.) These curves are qualitatively similar to the exact, classical coplanar O_2 - Ar solutions of Kuksenko and Lesov[15] and of Benson

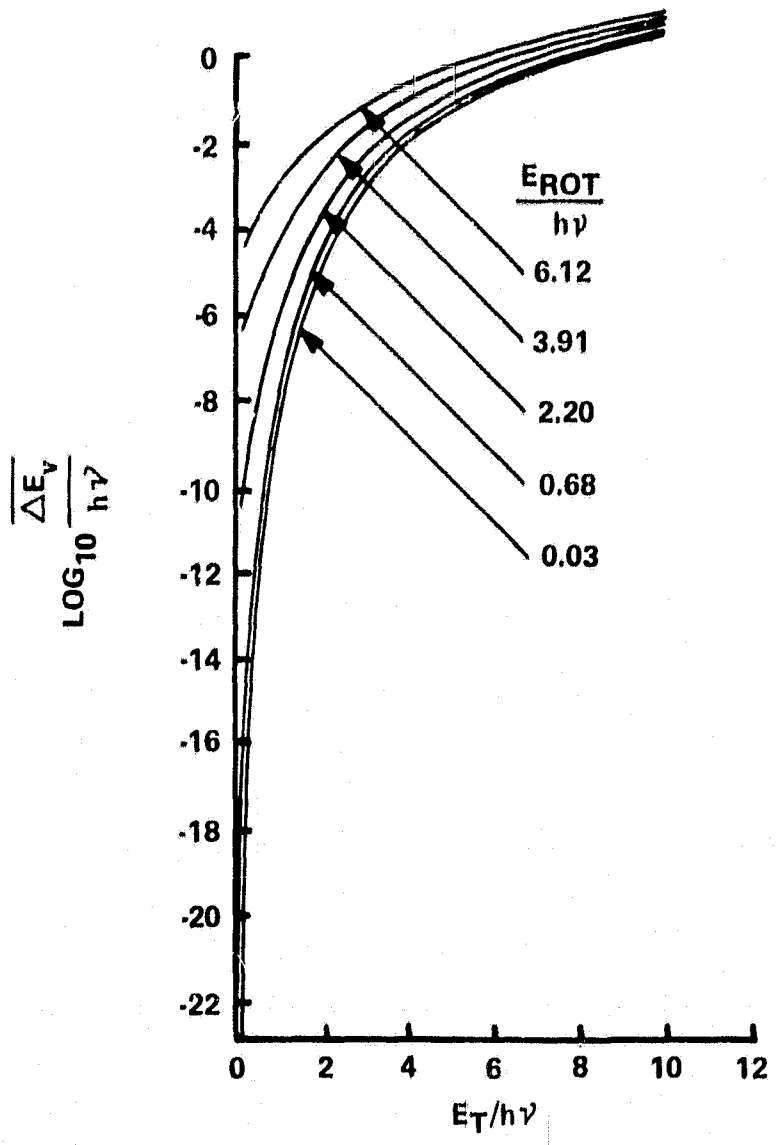

Figure 15 CLASSICAL ENERGY ΔE_v TRANSFERRED TO VIBRATIONAL MODE OF O_2 DURING COLLISION WITH Ar, AS A FUNCTION OF TRANSLATIONAL ENERGY. PLOTS FOR VARYING AMOUNTS OF O_2 ROTATIONAL ENERGY. APPROXIMATE APPROXIMATE ANALYTICAL MODEL (SEC. 5)

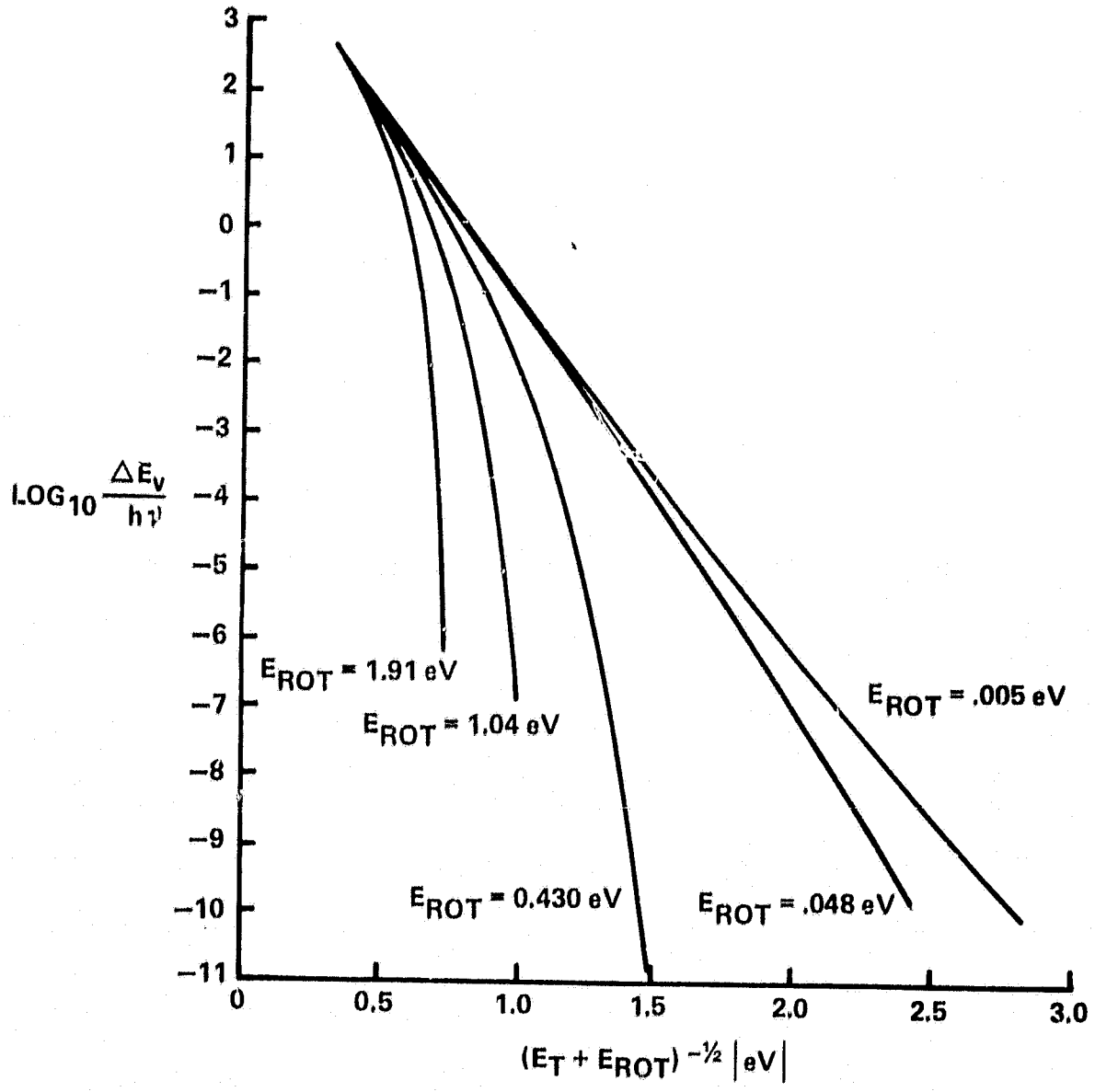

Figure 16 CLASSICAL ENERGY ΔE_v TRANSFERRED TO VIBRATIONAL MODE OF O_2 DURING COLLISION WITH Ar, AS A FUNCTION OF $[E_T + E_{ROT}]^{-1/2}$. PLOTS FOR VARYING AMOUNTS OF O_2 ROTATIONAL ENERGY. APPROXIMATE ANALYTICAL MODEL (SEC. 5)

and Berend.[4*] These curves also demonstrate the rotational effects discussed in the preceding paragraph. Figure 15 plots the results in a way similar to the plots of Kuksenko and Losev; Fig. 16 is similar to the plot given by Benson and Berend. It is found that our analytic zero-impact parameter case is $O[10^1]$ larger than the machine calculated ΔE_v's of Ref 15 which were averaged over impact parameter. Some of this difference is undoubtedly due to the effect of non-zero impact parameter, but the analytical result, Eq (5-18), definitely greatly over estimates the magnitude of ΔE_v, particularly for $E_T \geq E_R$ (see discussion below).

The curves in the preceding figures were prepared for $b = 0$. Taking $b = 0$ also implies $\dot{\phi}_o = \frac{V_\infty b}{R_o^2} = 0$. For $b \neq 0$, $\dot{\phi}_o \neq 0$. The physical interpretation of the effect of nonzero $\dot{\phi}$ is straightforward: depending on the sign of $\dot{\phi}_o$, relative to ω_R, the collision partner's motion can either add or subtract a component to the effective collision velocity created by the rotational motion. Figure 17 is a plot of ΔE_v (calculated from Eq (5-18) versus impact parameter, b, for the $\omega_R = 0$ case. It appears that a reasonably correct modeling of the dependence of ΔE_v on impact parameter can be obtained.

Finally, a comparison is possible with the (more exact) ΔE_v's calculated using the decoupled normal mode (DNM) classical model of Section 2. Figure 18 shows such a comparison, for CO_2 symmetric stretch-Ar collisions. It should first be noted that any decoupling approximation will involve a violation of energy conservation. This is reflected in Fig. 18, where both sets of curves exhibit a high energy failure, in the sense that when the available energy $E_T + E_R >> h\nu$, then $\Delta E_v > E_T + E_R$, violating energy conservation. The effect is, however, much more marked in the approximate analytical calculation; agreement with the DNM model is best for cases wherein $E_R >> E_T$, as might be expected from the decoupling assumptions which

---

* There is however, one important effect of rotation which the analytical treatment is unable to model even qualitatively. This is the dependence of the classical turning point location on the ratio of translational to rotational energies, and is discussed by Benson and Berend.[4] This effect causes a greater influence of rotation at higher translational energies than is shown by the present result.

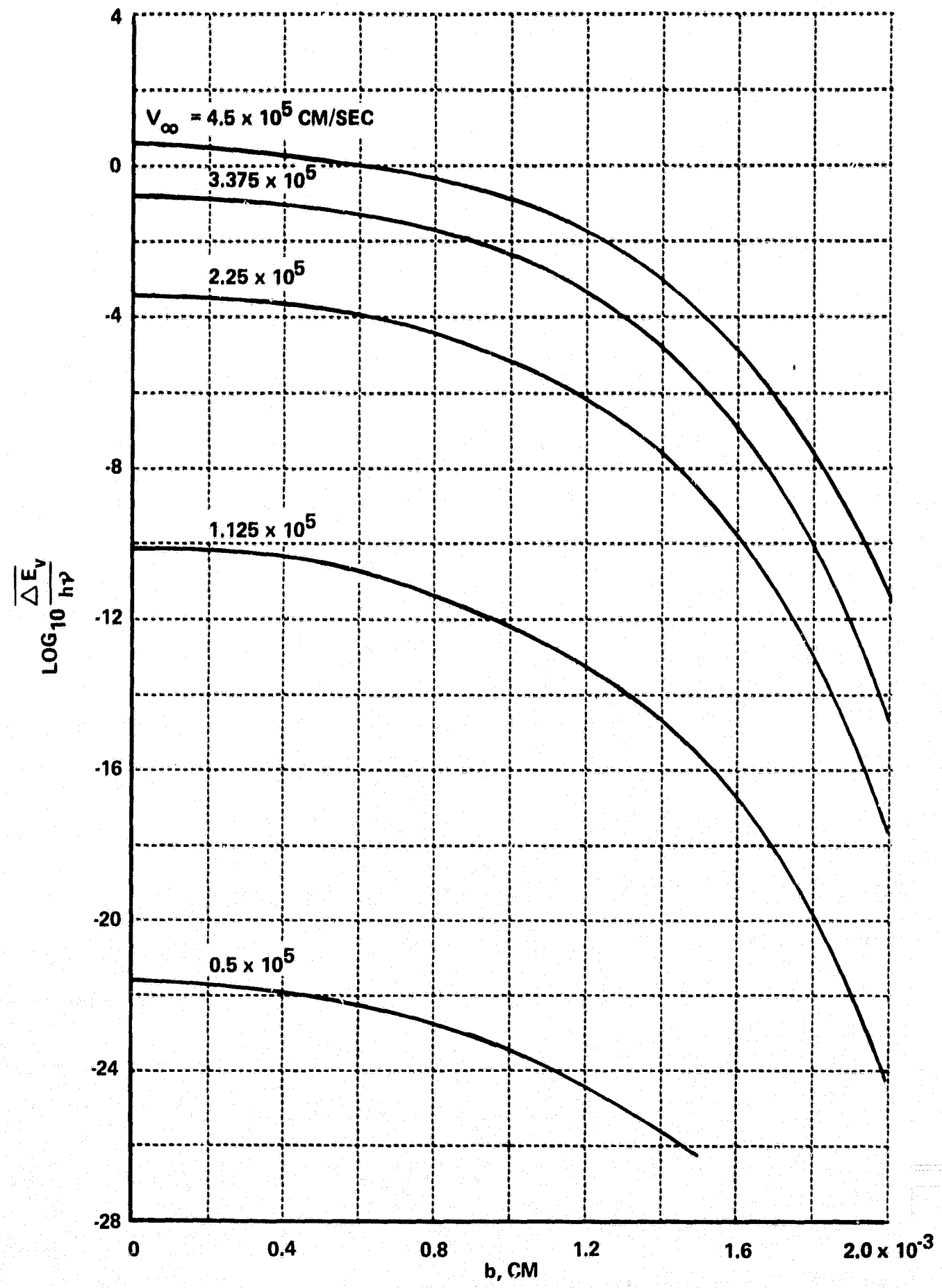

Figure 17 CLASSICAL ENERGY ΔE_v TRANSFERRED TO VIBRATIONAL MODE OF O_2 DURING COLLISION WITH Ar, AS A FUNCTION OF IMPACT PARAMETER. PLOTS FOR ZERO ROTATIONAL ENERGY AND VARYING AMOUNTS OF TRANSLATIONAL ENERGY. APPROXIMATE ANALYTICAL MODEL (SEC. 5)

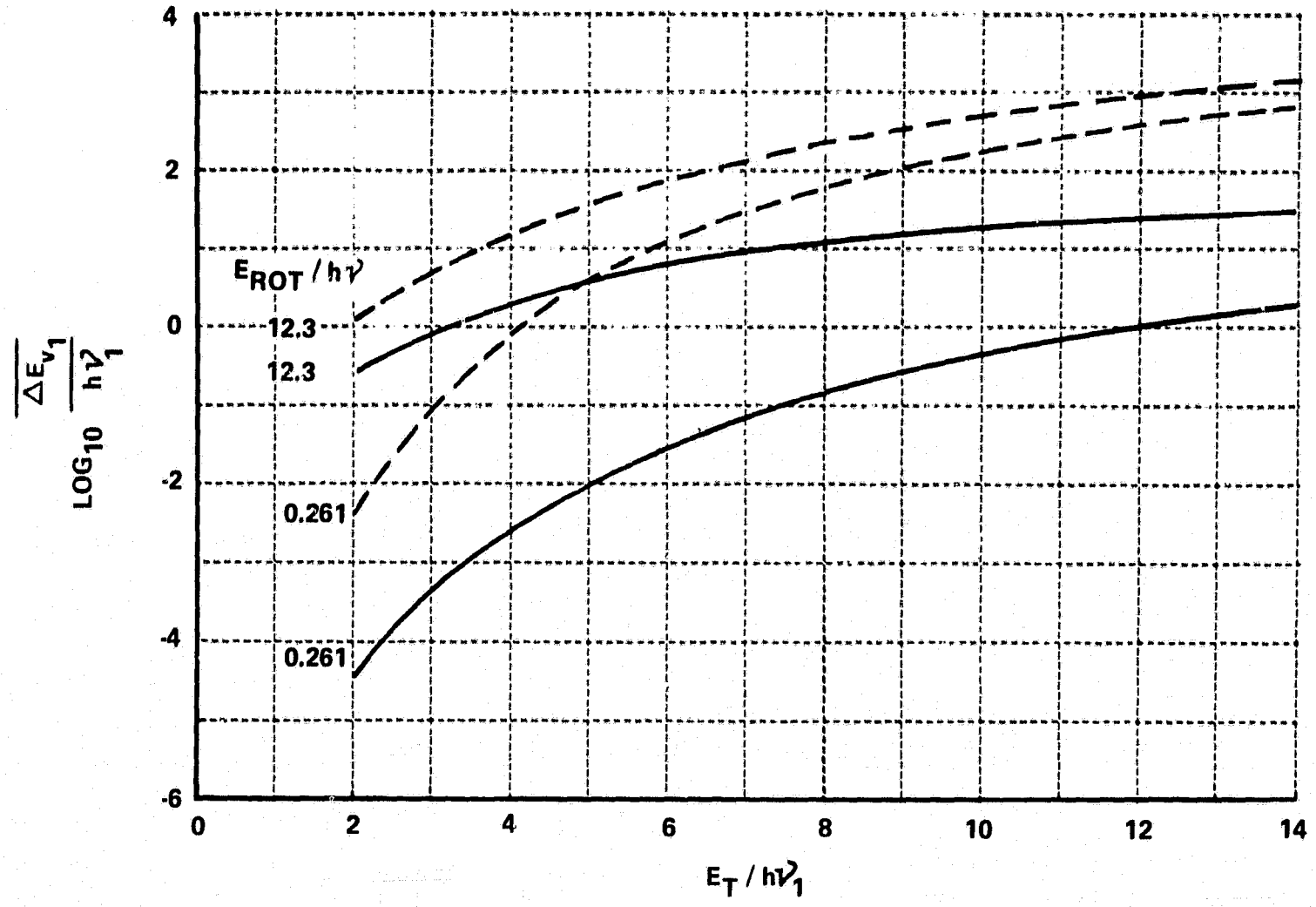

Figure 18 ΔE_v TRANSFERRED TO SYMMETRIC STRETCHING MODE OF CO_2 DURING COLLISION WITH Ar. COMPARISON OF APPROXIMATE ANALYTIC CALCULATION AND MACHINE (DNM) CALCULATION FOR b = 0.

led to the analytical result, Eq (5-18). It is this feature which limits the usefulness of the analytic result to investigation of qualitative features only.

5.2 THERMAL AVERAGING OF COLINEAR V-T TRANSITION PROBABILITIES

A further analytic study was undertaken in support of the thermal averaging calculations treated in Section 3. As discussed in Section 3, the V-T transition probabilities as given by Eq (2-13) must be averaged over a thermal distribution of initial trajectory parameters to obtain the dependence of the V-T excitation cross sections on temperature. Generally, this is to be accomplished by machine integration (see Section 3). However, as a guide to such calculations, this section discusses analytic thermal integration of the transition probabilities of Eq (2-13), for a simple colinear interaction.

Equation (2-13) gives the quantum mechanical transition probability for a collisionally induced transition between the states o , n of a harmonic oscillator to be:

$$P_{on} = \frac{e^{-\epsilon_i}\,\epsilon_i^n}{n!} \tag{5-19}$$

Reference 3 discusses the analytic evaluation of ϵ_i for the colinear collision of an atom A with a molecule B-C , initially in its ground vibrational state.* Substitution of the analytic result for ϵ_i into Eq (5-19) gives:

$$P_{on}(V) = \frac{1}{n!}\,A^n\,V^{2n}\,\operatorname{sech}^{2n}\frac{2WL}{V}\,e^{-AV^2\operatorname{sech}^2\frac{2WL}{V}} \tag{5-20}$$

where

V = relative translational velocity of the atom and molecule

---

* The potential used to obtain this result is based on an expansion of the intermolecular potential II of Ref 3; this potential, first used by Rapp and Sharp,[37] is quite similar to an exponentially repulsive interaction between the A and B atoms.

$$A = \frac{2}{\hbar\omega}\,\frac{\tilde{m}^2}{\mu}\left(\frac{m_c}{m_B + m_c}\right)^2$$

ω = oscillator radial frequency

μ = oscillator reduced mass = $\dfrac{m_B\, m_c}{m_B + m_c}$

$\tilde{m}$ = system reduced mass = $\dfrac{m_A (m_B + m_c)}{m_A + m_B + m_c}$

L = exponential range of atom-molecule potential

If this transition probability is averaged over a one-dimensional Maxwellian distribution of translational velocities, there is obtained

$$P_{on}(T) = \frac{1}{n!}\, A^n\, \frac{\tilde{m}}{KT} \int_{-\infty}^{\infty} V^{2n+1} \exp -\left\{2n \ln\left[\cosh\left(\frac{2\omega L}{V}\right)\right] + \frac{\tilde{m}V^2}{2KT} + AV^2 \operatorname{sech}^2\left(\frac{2\omega L}{V}\right)\right\} dV \qquad (5\text{-}21)$$

The integrand of this expression is sharply peaked near the maximum of the exponential factor. Integration is accomplished by expanding the argument of the exponential about its minimum value. This minimum value is easily shown to occur at a value of $V = V_c$ given by the solution of the following transcendental equation:

$$\frac{\tilde{m}V_c^3}{KT} = 4n\omega L \tanh\left(\frac{2\omega L}{V_c}\right) - 2AV_c^2 \operatorname{sech}^2\left(\frac{2\omega L}{V_c}\right)\left[V_c + 2\omega L \tanh\left(\frac{2\omega L}{V_c}\right)\right]. \qquad (5\text{-}22)$$

For those cases (corresponding to the lower temperatures) in which $\frac{2\omega L}{V_c} \gg 1$, an approximate value of $V_c \approx V_m$ is obtained by taking $\tanh\left(\frac{2\omega L}{V_c}\right) \sim 1$, $\operatorname{sech}\left(\frac{2\omega L}{V_c}\right) \sim 0$, giving

$$V_m = \left(\frac{4n\omega L KT}{\tilde{m}}\right)^{1/3} \qquad (5\text{-}23)$$

For $n = 1$, this last result is the Schwartz-Slawsky-Herzfeld formula for the critical velocity. At the higher temperatures, however, Eq (5-23) is inaccurate, and the complete solution of Eq (5-22) must be used. Figures 19 and 20 give a comparison of the approximate (Eq 5-23) and exact solutions of Eq (5-22) using the molecular parameters of the asymmetric stretching mode and the bending mode of CO_2. (Solution of Eq (5-22) was accomplished using a machine Newton-Raphson iteration.) It is seen that at the higher temperatures, the critical velocity is less than the values given by Eq (5-23). "Softer" vibrational

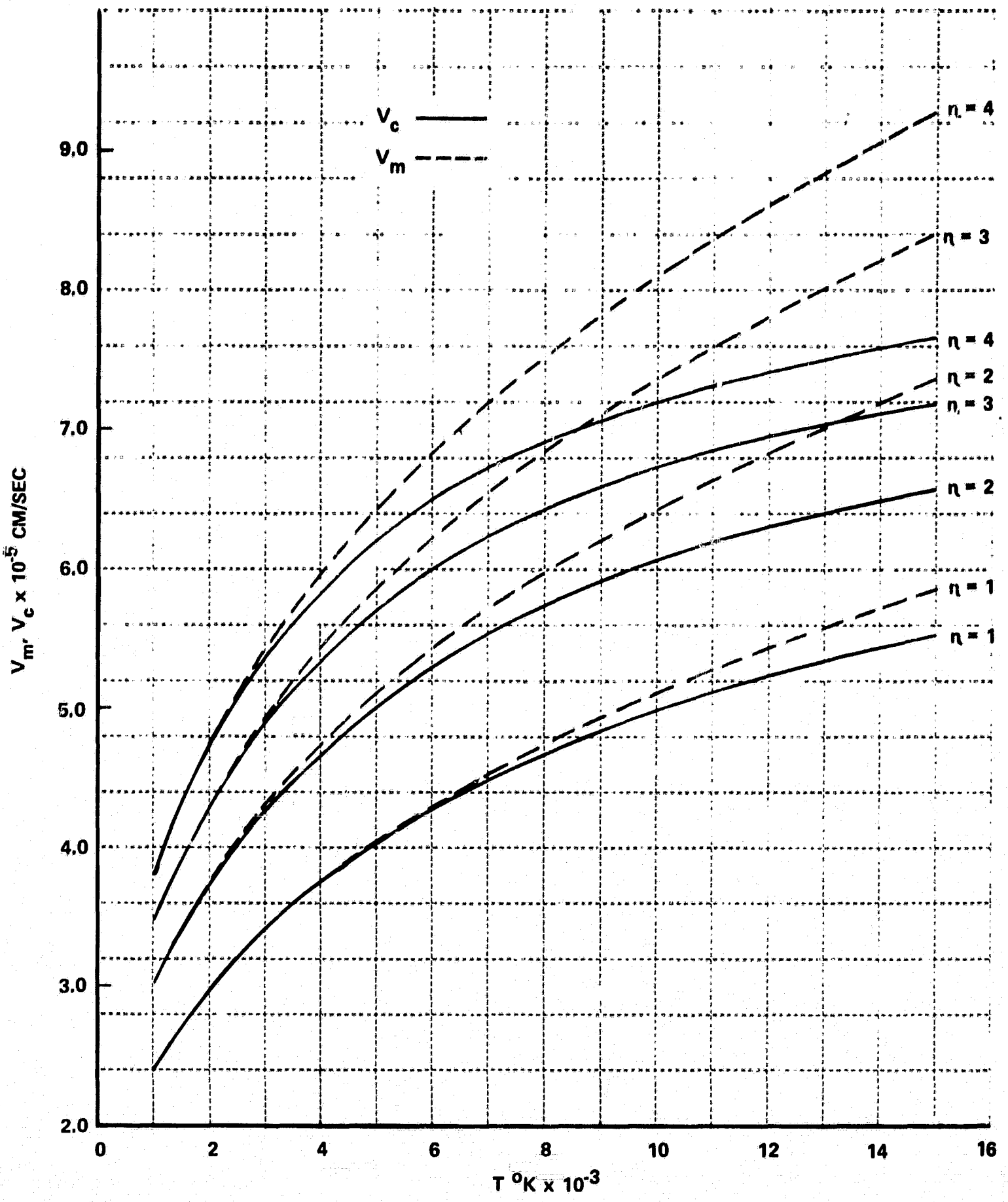

Figure 19 CO_2 **ASYMMETRIC STRETCHING MODE CRITICAL VELOCITIES VS. TEMPERATURE**

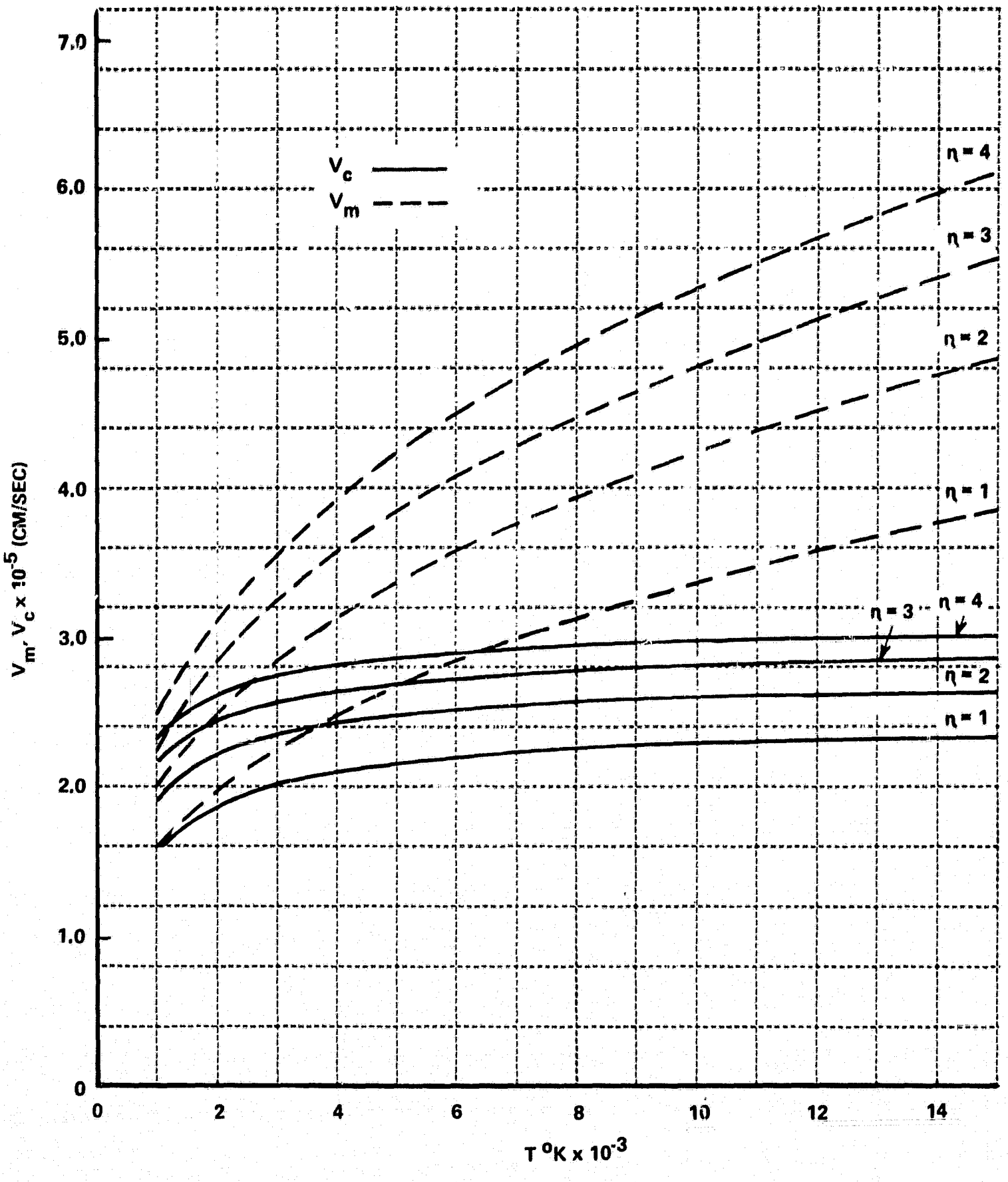

Figure 20 CO_2 BENDING MODE — CRITICAL VELOCITIES VS. TEMPERATURE

modes, characterized by lower frequencies, show considerable divergence between V_c and V_m .

Having determined V_c , the argument of the exponent in Eq (5-21) is expanded in powers of $V-V_c$ and terms beyond $(V-V_c)^2$ are neglected. Equation (5-21) can then be integrated analytically, yielding the result:

$$P_{on}(T) = \left[\frac{1}{n!} A'' \frac{\tilde{m}}{KT} \left(\frac{2\pi}{f''(V_c)}\right)^{1/2} V_c^{2n+1} e^{-f(V_c)}\right] \sum_{\nu=0}^{n} \frac{(2n+1)!}{(2n+1-2\nu)!\nu!} \left(\frac{1}{2V_c^2 f''(V_c)}\right)^{\nu} \tag{5-24}$$

where $f(V)$ is the argument of the exponent in Eq (5-21).

Equation (5-24) is displayed, again for the asymmetric stretching and the bending modes of CO_2 in Figs. 21 and 22. It is seen that even at 15,000°K, the probability of multiple jumps is smaller than the single jump probability. For almost all cases of interest, the sum appearing in Eq (5-24) is very close to one, terms beyond the $\nu=0$ term being negligibly small. At sufficiently high temperatures, however, $P_{on}(T)$ will approach asymptotic values, as the distribution of molecular velocities becomes less sharply peaked. In this limit, V_c goes to a limiting value independent of T , given by the maximum of the $VP_{on}(V)$ curves. This effect is observable near 15,000°K in the curves for the CO_2 bending mode, Fig. 22. For a stiffer mode, the transition probabilities will asymptote at some higher temperature. In this limit $P_{on}(T)$ becomes proportional to T^{-1};

$$P_{on}(T) \sim \frac{A^n}{n!} \frac{\tilde{m}}{KT} \int_0^{\infty} V^{2n+1} \operatorname{sech}^{2n}\left(\frac{2\omega L}{V}\right) e^{-AV^2 \operatorname{sech}^2\left(\frac{2\omega L}{V}\right)} dV.$$

Numerical comparison of the exact and the approximate integrands shows that the steepest descent evaluation still remains valid in the high temperature region. It is found that P_{o1}/P_{on} can become less than $1/n$ as $T \to \infty$. The energy transferred in a $o \to n$ transition is given by $\Delta E_v P_{on} = \hbar \omega_n P_{on}$. In the high temperature limit, therefore, the model of Ref 3 predicts that multiple quantum jump transitions will become quite important for energy transfer.

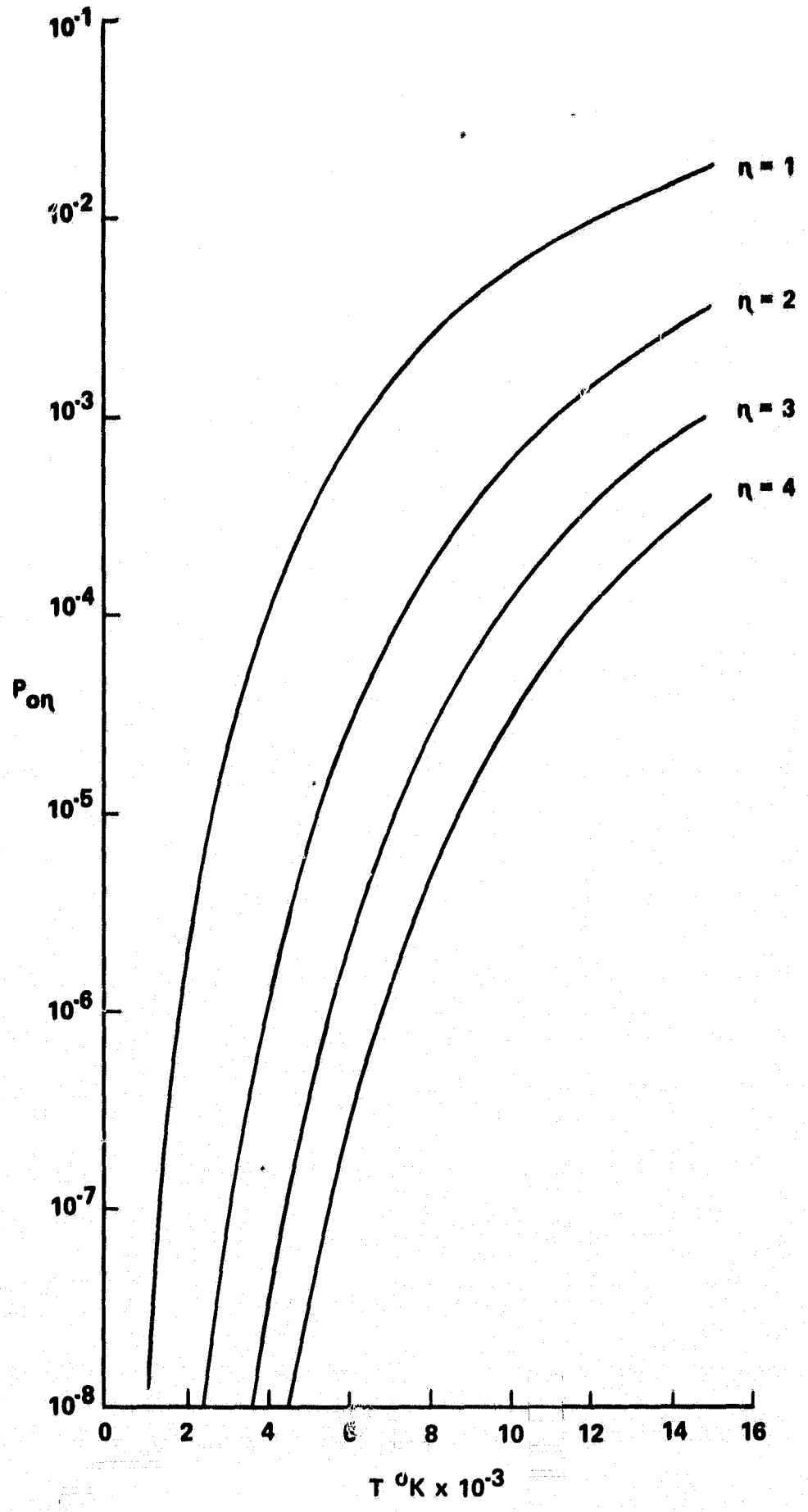

Figure 21 CO_2 **ASYMMETRIC STRETCHING MODE – V-T NON-PERTURBATIVE TRANSITION PROBABILITIES**

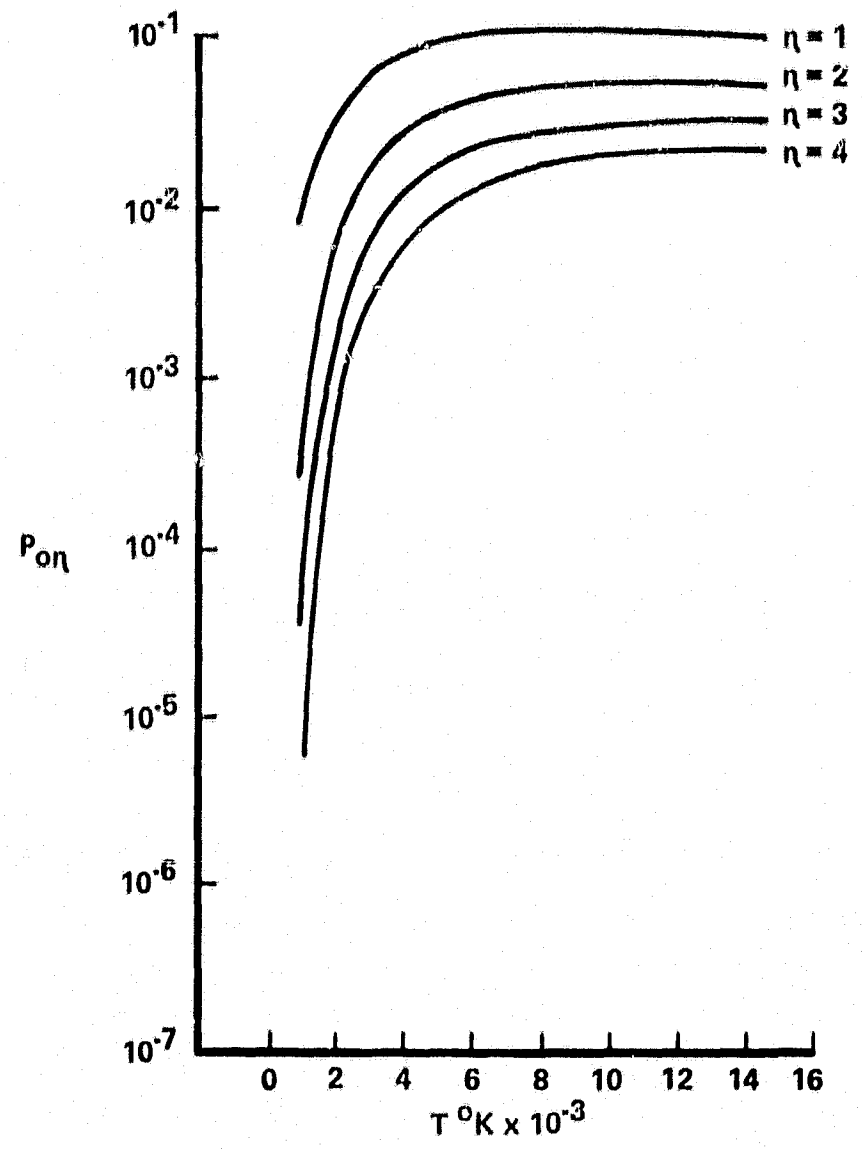

Figure 22 CO_2 BENDING MODE - V-T NON-PERTURBATIVE TRANSITION PROBABILITIES

6. INTERMODE COUPLING MODEL

The calculations discussed in the preceding sections utilize a normal-mode model of the CO_2 molecule, with no coupling among the various CO_2 modes. It is well known, however, that the observed IR and Raman spectra of CO_2 are not entirely consistent with a purely normal-mode theoretical model of the vibrational energy states. The energies of some kinetically important CO_2 states can be predicted only if one considers anharmonicity coupling between normal-mode states having comparable energies. This mechanism is the well-known Fermi resonance coupling, and it gives rise to a "mixing" of some of the normal-mode vibrational wave functions. A general treatment of CO_2 vibrational excitation should consider transitions between these mixed states. This section is concerned with a model which will enable V-T transition probabilities to be calculated for transitions among "mixed" states. The present model treats the collision as a time-dependent perturbation acting on CO_2 vibration. The unperturbed CO_2 vibrational motion includes intermode coupling due to anharmonicity.

The Hamiltonian for the normal, uncoupled CO_2 modes can be written:

$$H_V = \frac{\hbar}{2}\left[\omega_1 \frac{\partial^2}{\partial r_1^2} + \omega_2\left(\frac{1}{r_2}\frac{\partial}{\partial r_2}\left(r_2\frac{\partial}{\partial r_2}\right) + \frac{1}{r_2^2}\frac{\partial^2}{\partial \gamma^2}\right) + \omega_3\frac{\partial^2}{\partial r_3^2}\right]$$

$$- \frac{\hbar}{2}\left[\omega_1 r_1^2 + \omega_2 r_2^2 + \omega_3 r_3^2\right] , \qquad (6\text{-}1)$$

where r_i are dimensionless coordinates proportional to the normal displacements, and $\omega_i = 2\pi\nu_i$ are the circular vibrational frequencies.

The first order anharmonicity terms are

$$U_1 = 2\pi\hbar\left[\alpha_{111} r_1^3 + \alpha_{122} r_1 r_2^2 + \alpha_{133} r_1 r_3^2\right] . \qquad (6\text{-}2)$$

The solution of the following equation for CO_2 :

$$(H_{\nu} + U_1)\,\psi = E\,\psi \quad , \tag{6-3}$$

is treated in standard references[38, 39, 22] where wave functions and energy levels are obtained using first order time-independent perturbation theory for degenerate levels. The wave functions, ψ_n , are found, to zeroth order in the approximation, to be linear combinations of the normal mode wave functions:

$$\psi_n \approx \psi_n^{\{0\}} = \sum_{k=0}^{g} c_{nk}^{(0)}\ \psi_k^{(0)} \quad , \tag{6-4}$$

where g is the order of the Fermi resonance degeneracy, and the normal mode wave functions $\psi^{(0)}$ are given by:

$$\psi^{(0)} = u_1(r_1)\ u_3(r_3)\ R^{\nu_2 \ell}(r_2)\ e^{\pm i \ell \gamma} \quad . \tag{6-5}$$

Here, $u(r_i)$ are the standard SHO wave functions:

$$u_i(r_i) = N_{\nu_i}\ e^{-\frac{1}{2} r_i^2}\ H_{\nu_i}(r_i) \quad ,$$

$$N_{\nu_i}^2 = \frac{1}{\sqrt{\pi}\ 2^{\nu_i}\ \nu_i!} \quad ,$$

$H_{\nu_i}(r_i)$ is the ν_i^{th} Hermite polynomial of argument r_i .

The remaining part of the wave function, $R^{\nu_2 \ell}(r_2)\, e^{\pm i \ell \gamma}$, is the solution for the two-dimensional isotropic harmonic oscillator in polar coordinates (r_2 , γ):

$$R(r_2)^{\nu_2 \ell}\, e^{\pm i \ell \gamma} = \left[k!\right]^{1/2} \left[(\ell + k)!\right]^{-1/2} \pi^{-1/2}\, r_2^{\ell}\, e^{-r_2^2/2}\, L_k^{\ell}(r_2^2)\, e^{\pm i \ell \gamma} \quad ,$$

where $k \equiv (\nu_2 - \ell)/2$. $L_k^{\ell}(r_2^2)$ is the associated Laguerre polynomial of argument r_2^2 .

The $C_{nk}^{(0)}$'s are found using standard time-independent perturbation theory for degenerate levels. The $C_{nk}^{(0)}$'s are so chosen that the wave functions $\psi_n^{\{0\}}$ are orthonormal.

The energy levels for the lower CO_2 states are shown in Fig. 23. The wave functions corresponding to the lowest nine states are given in the following table:

State designation		Wave function	Energy, cm^{-1}
n	$(V_1\ V_2^{\ell}\ V_3)$	$\psi_n^{\{0\}} / \psi_0^{\{0\}} = \pi\, e^{\frac{1}{2}(r_1^2+r_2^2+r_3^2)}\ \psi_n^{\{0\}}$	E_n
0	$(0\ 0^{\circ}\ 0)$	1	0
1	$(0\ 1'\ 0)$	$r_2\, e^{\pm i\gamma}$	667
2	$(0\ 2^{\circ}\ 0)$	$0.648\sqrt{2}\, r_1 - 0.766(1-r_2^2)$	1285
3	$(1\ 0^{\circ}\ 0)$	$0.766\sqrt{2}\, r_1 + 0.648(1-r_2^2)$	1388
4	$(0\ 2^2\ 0)$	$\frac{1}{\sqrt{2}}\sqrt{2}^{\,2}\, e^{\pm 2i\gamma}$	1335
5	$(0\ 3'\ 0)$	$0.743\frac{1}{\sqrt{2}}(2r_2-r_2^3)e^{\pm i\gamma} + 0.669\sqrt{2}\, r_1 r_2\, e^{\pm i\gamma}$	1932
6	$(1\ 1'\ 0)$	$0.669\frac{1}{\sqrt{2}}(2r_2-r_2^3)e^{\pm i\gamma} - 0.743\sqrt{2}\, r_1 r_2\, e^{\pm i\gamma}$	2077
7	$(0\ 3^3\ 0)$	$\frac{1}{\sqrt{6}}\, r_2^{\,3}\, e^{\pm 3i\gamma}$	2003
8	$(0\ 0^{\circ}\ 1)$	$\sqrt{2}\, r_3$	2349

The states in Fermi resonance are linked by braces. It is the spectroscopic convention to assign to these mixed levels the term designation of their larger component.

We now consider the behavior of the above system under the action of a time-dependent perturbation of the form:

$$V = f_0(t) + \sum_{i=1}^{3} f_i(t)\, r_i + \sum_{i,j=1}^{3} g_{ij}(t)\, r_i r_j + \cdots \qquad (6\text{-}6)$$

As discussed in previous sections, the influence of a collision can be represented by a potential of this form.

Using standard methods, the solution of the wave equation for the

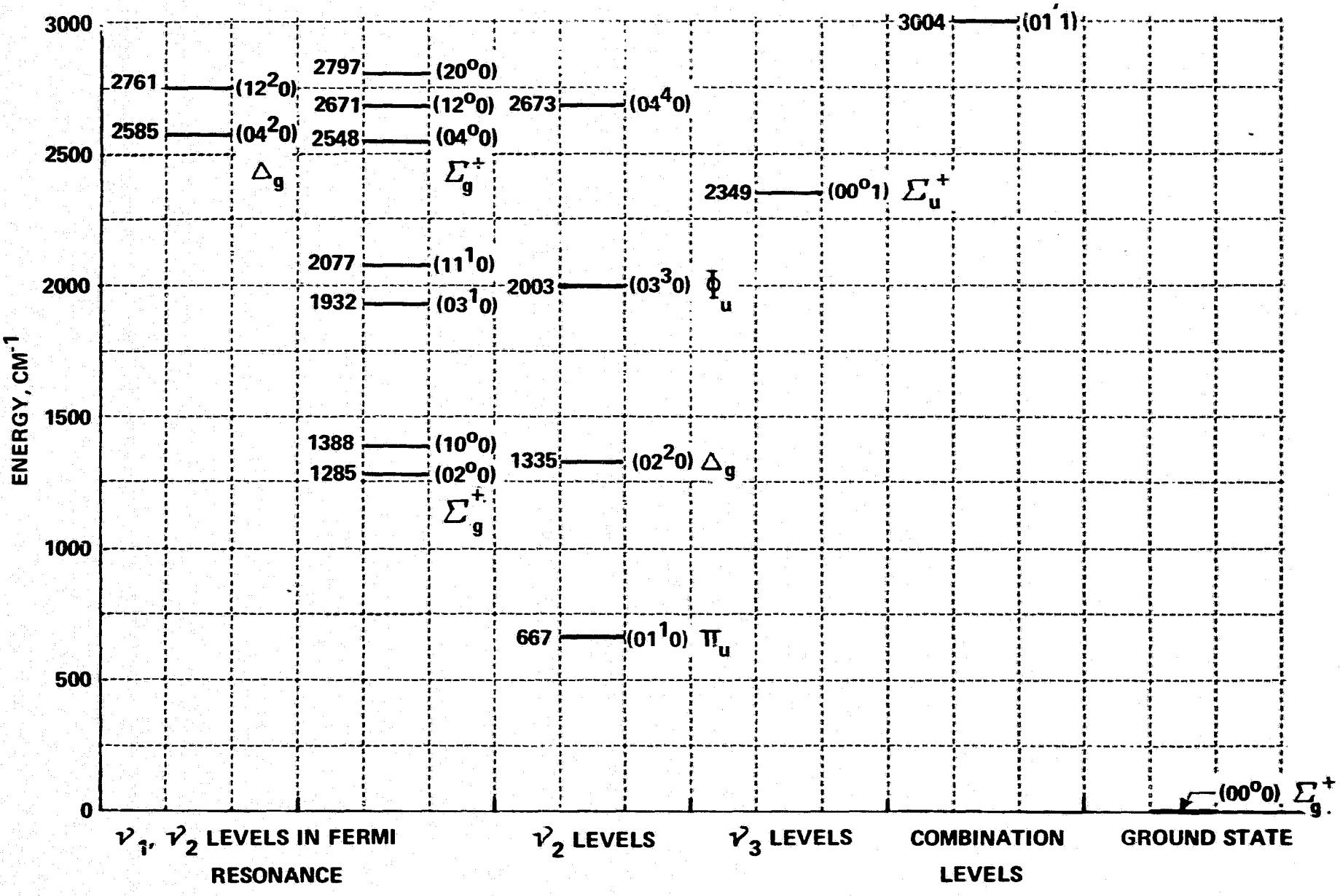

Figure 23 CO_2 ENERGY LEVELS

perturbed system:

$$(H_v + U_1 + V)\,\Psi = i\hbar\,\frac{\partial \Psi}{\partial t} \tag{6-7}$$

can be rephrased in a completely equivalent way as a problem in finding the coefficients $b_{mn}(t)$, where

$$\Psi_m = \sum_n b_{nm}(t)\,\psi_n^{\{0\}}\,e^{-iE_n t/\hbar} \quad . \tag{6-8}$$

$\psi_n^{\{0\}}$ are the combination wave functions given by Eq (6-4). The coefficients b_{mn} are determined exactly by the solution of the first order equations:

$$\dot{b}_{mn} = -\frac{i}{\hbar}\sum_k \langle n|V|k\rangle\, b_{mk}\, e^{i\omega_{nk}t} \tag{6-9}$$

where $n = 0, 1, 2, \ldots$

$$\langle n|V|k\rangle \equiv \int_{\gamma=0}^{2\pi}\int_{r_3=\infty}^{\infty}\int_{r_2=0}^{\infty}\int_{r_1=-\infty}^{\infty} \psi_n^{\{0\}*}\, V\, \psi_k^{\{0\}}\, r_2\, dr_1\, dr_2\, dr_3\, d\gamma \quad , \tag{6-10}$$

$$\omega_{nk} \equiv (E_n - E_k)/\hbar \quad .$$

Equations (6-9) are the so-called interaction representation, and are completely equivalent to the wave Eq (6-7), no small perturbation approximation having as yet been introduced. If the CO_2 molecule is initially in state m before collision ($t = -\infty$), $|b_{mn}(t)|^2$ is the probability that it will be in state n at time t.

The evaluation of the matrix elements $\langle n|V|k\rangle$ appearing in Eq (6-9) becomes increasingly cumbersome as higher order terms are retained in V (Eq (6-6)). The difficulty does not lie in performing the integration over the oscillator coordinates S_1, S_2, S_3, γ, however. At least for the lower CO_2 states, the wave functions, as given in Table 1, are quite simple, and these integrals can readily be evaluated in closed form. The source of complexity lies in the evaluation of the time-dependent coefficients, $f_i(t)$, $g_{ij}(t)$, etc. These coefficients involve derivatives of the intermolecular potential with respect to the vibrational coordinates. Only first order derivatives

appear in $f_i(t)$, but second order derivatives occur in $g_{ij}(t)$, etc. The degree of complexity is strongly dependent on the functional form chosen for the intermolecular potential. The first order coefficient, $f_i(t)$, and the second order coefficients, $S_{ij}(t)$, have been evaluated for the point center, pairwise additive exponential interaction potential used in the normal mode calculations of Section 2.*

It is planned to obtain machine solutions of Eq (6-9), including the nine states listed in Table 1, which contains all CO_2 states having a characteristic temperature $\leq$ 3500°K. These include the states important in CO_2 laser action. Sharp and Rapp[40] have programed equations similar to (6-9) and retained up to ten coupled states, using a Runge-Kutta routine. It, therefore, appears feasible to make such multistate calculations, although an investigation is being conducted to determine the most efficient machine computational procedure. In the remaining paragraphs of this section, some of the specific features and difficulties of this formulation are discussed.

Table 2 gives the matrix elements $\langle n|V|k\rangle$ including only the linear terms in V. Two significant features can be seen from these matrix elements:

i) It is found that the interaction potential V removes the l-doubling degeneracy of the $V_2 > 0$ states. In Table 2, the $l > 0$ states are primed, the $l < 0$ states are doubly primed. It is to be expected that the collisional interaction will remove the l degeneracy, inasmuch as the interaction depends on the direction of rotation of the bending plane of the CO_2 molecule. It should be noted that this feature effectively increases the number of states appearing in Eqs (6-9).

ii) Examination of Table 2 also shows that several states that are close energetically have zero coupling matrix elements, in the linear approximation to V. For example, the laser states,

---

* Both f_i & g_{ij} are expressed as explicit functions of the trajectory parameters, R, Θ, Φ, α, β. These parameters are functions of time, and thus f_i & g_{ij} are implicit functions of t.

TABLE 2 INTERACTION MATRI

	0	1'	1''	2	3	4'	4''	5'
0	$\hat{f}_0$	$\hat{f}_2/2$	$\hat{f}_2^*/2$	$\hat{f}_1/2$	$\hat{f}_1/2$	0	0	0
1'		$\hat{f}_0$	0	$2^{-3/2}\,\hat{f}_2^*$	$-2^{-3/2}\hat{f}_2^*$	$2^{-1/2}\,\hat{f}_2$	0	$0.472\,\hat{f}_1$
1''			$\hat{f}_0$	$2^{-3/2}\,\hat{f}_2$	$-2^{-3/2}\,\hat{f}_2$	0	$2^{-1/2}\,\hat{f}_2^*$	0
2				$\hat{f}_0$	0	0	0	$-0.134\,\hat{f}_2$
3					$\hat{f}_0$	0	0	$0.608\,\hat{f}_2$
4'					$\hat{f}_0$	0		$-0.371\,\hat{f}_2^*$
4''						$\hat{f}_0$	0	
5'							$\hat{f}_0$	
5''								
6'								
6''								
7'								
7''								
8								

NOTE:

$$\hat{f}_2 = \hat{f}_{2b} + i\hat{f}_{2a}$$

IATRIX FOR LINEARLY FORCED CO_2

5′	5″	6′	6″	7′	7″	8	TERM DESIGNATION
0	0	0	0	0	0	$\hat{f}_3/\sqrt{2}$	(0 0°0)
.472 $\hat{f}_1$	0	$-0.524\hat{f}_1$	0	0	0	0	(0 1′0) +
0	0.472 $\hat{f}_1$	0	$-0.524\hat{f}_1$	0	0	0	(0 1′0) −
.134 $\hat{f}_2$	$-0.134\hat{f}_2^*$	$-0.072\hat{f}_2^*$	$0.072\hat{f}_2^*$	0	0	0	(0 2°0)
.608 $\hat{f}_2$	$0.608\hat{f}^*$	$0.598\hat{f}_2$	$0.072\hat{f}_2^*$	0	0	0	(1 0°0)
.371 $\hat{f}_2^*$	0	$-0.335\hat{f}_2^*$	0	$\frac{1}{2}\sqrt{3}\hat{f}_2$	0	0	(0 2²0) +
0	$-0.371\hat{f}_2$	0	$-0.335\hat{f}_2$	0	$\frac{1}{2}\sqrt{3}\hat{f}_2^*$	0	(0 2² 0) −
$\hat{f}_0$	0	0	0	0	0	0	(0 3′0) +
	$\hat{f}_0$	0	0	0	0	0	(0 3′0) −
		$\hat{f}_0$	0	0	0	0	(1 1′0) +
			$\hat{f}_0$	0	0	0	(1 1′0) −
				$\hat{f}_0$	0	0	(0 3³0) +
					$\hat{f}_0$	0	(0 3³0) −
						$\hat{f}_0$	(0 0°1)

2

($00^{\circ}1$) and ($10^{\circ}0$), are not coupled by the linearized potential. Many important collisionally induced intramolecular V-V couplings only occur if quadratic terms such as $g_{ij} S_i S_j$ are included in the potential.* Therefore, it appears desirable to include the contribution of second order terms to V in calculating the matrix elements.

Thus two major computational problems in obtaining machine solutions of Eq (6-9) are now apparent. One problem arises from the additional number of participating states, due to the ℓ -splitting discussed in i). The second problem is created by the need for including quadratic terms in V, as discussed in ii).** Both these features increase demand on the amount of machine computation necessary to obtain a solution. While the number of Runge-Kutta integration steps, for a given collisional trajectory, would not be greater than that in the normal mode program used in Section 2, the number of operations per step would be greatly increased. We are presently studying ways to minimize this problem.

---

* It should be noted, however, that in a multistate calculation, such as contemplated here, collisionally induced transitions still occur between states for which $\langle n|V|k\rangle = 0$. Only in first order perturbation theory does $\langle n|V|k\rangle = 0$ imply $P_{nk} = 0$.

** Both these problems arise because of the general, three-dimensional treatment of the molecular collision. For coplanar cases, the ℓ -splitting problem disappears, and the calculation of the second order coefficients g_{ij} is greatly simplified.

7. SUMMARY

This interim report has presented the formulation and analyses of models which will allow calculation of thermally averaged cross sections for the vibrational excitation of CO_2. The basic process modeled is energy transfer from the translational and rotational modes of the gas into the vibrational modes of the CO_2 molecule--what is called, in the report, a V-T process. The archetype of such a process occurs in the adjustment to thermal equilibrium which takes place behind gas-dynamic shocks. Major emphasis to date has been placed on calculating trajectories and energy transfer for the inelastic collision of a structureless (i.e., nonvibrating, nonrotating, spherically symmetric) particle with a CO_2 molecule. These results, in terms of inelastic cross sections, are then used with a Monte Carlo scheme to compute thermally averaged transition probabilities for vibrational excitation.

Previous analyses of inelastic collisions of a CO_2 molecule with a second particle have suffered from at least one of the following restrictions. (1) The calculation of the inelastic cross section has been restricted to that of first-order perturbation theory. (2) The nonspherical nature of the potential has been neglected. (3) The effect of rotation of the CO_2 molecule on the energy transfer has been neglected. (4) The influence of vibrational bending of the CO_2 molecule on the energy transfer has been neglected. (5) Intermode coupling during the collision has been ignored. The present studies have been directed toward including these features of the collision in the analysis.

Modeling and analysis of the V-T energy transfer process is treated principally in Sections 1-3. The decoupled-normal-mode (DNM) model presented in these sections retains such features as a nonspherically symmetric intermolecular potential, the influence of molecular rotation, and the influence of the vibrational bending modes. The inclusion of these features is desirable for the specific case of CO_2 V-T excitation, wherein the role of the bending modes is expected to be significant.

As discussed in Section 1, any cross section calculation for the vibrational excitation of CO_2 currently must rely on empirically derived potential data. It is therefore mandatory that a model calculation of thermal V-T cross sections be sufficiently flexible to allow parametric investigation of the effects of various potential features, without requiring an impractical amount of machine computation time. The DNM model permits computation of the vibrational transition probabilities in such a sufficiently short time. This reduction in the computational time is achieved in two ways. First, the decoupling approximation reduces the number of initial trajectory parameters involved; in particular, the need for averaging over the various vibrational phases and energies is eliminated. Thus the dimensionality of the thermal cross-section integral (Eq. (3.1)) has been significantly reduced. A second feature of the DNM model is that V-T excitation of the various CO_2 modes can be examined independently. In particular, if the bending mode excitation is the basic V-T mechanism, then the V-T excitation of this mode can be calculated separately. A much larger amount of machine time would be required if the influence of all vibrational modes had to be incorporated into every trajectory calculation.

While treating the translational and rotational modes classically, the decoupling approximation, as used in the DNM model of Section 2, allows the retention of the quantized nature of the vibrational states. For the normal mode states of Section 2, quantum mechanical probabilities for collisionally induced vibrational transitions are obtained quite readily from the classical energy transfer expression (cf. Eq. (2-13)). When anharmonic coupling among the CO_2 modes is included in the analysis, calculation of the quantum mechanical transition probabilities is more complex (cf. Section 6). In either case, the decoupled semiclassical approach has the distinct advantage of permitting a realistic description of the strongly quantized vibrational energy modes, while using a computationally straightforward classical description of the rotational and translational motion of the system.

The theory developed in this study is meant to be applied over a wide range of kinetic temperatures. The DNM model is not restricted to low thermal velocities, as would be the case with a first-order quantum mechanical perturbation treatment.

The thermal averaging of transition probabilities based on the DNM model is treated in Section 3. The thermal cross-section integral is 6-fold for the general three-dimensional case, and 4-fold for coplanar cases. The problem of numerical integration is further complicated by the fact that the transition probabilities are quite sensitive functions of two of the integration variables, the initial translational and rotational energies.

Beyond colinear or spherically symmetric cases, the only thermal averaging of vibrational excitation cross sections is the recent work of Kuksenko and Losev.[15] That paper presents a calculation of a thermally averaged V-T cross section for the excitation of O_2 upon collision with Ar. The thermal cross-section integral appears to have been evaluated by straightforward numerical quadrature techniques; presumably a rather large number of trajectory calculations was required to obtain the results presented. Perhaps for this reason, variation of intermolecular potential parameters is limited to varying the exponential range parameter. Potential anisotropy was not varied.

For the present purposes, the Monte Carlo thermal averaging technique of Section 3 was developed. For multidimensional integrals, the Monte Carlo method offers the possibility of reducing the number of trajectory calculations required over more conventional numerical quadrature techniques. The number of points required for a given quadrature accuracy does not increase geometrically with the dimensionality of the integral. However, for vibrational excitation cross sections, wherein only collisions occurring in a rather narrow range of initial translational and rotational energies contribute to the integrand, some effective variance reducing technique is necessary. The variance reducing method discussed in Section 3 promises to be quite effective for the CO_2 vibrational excitation cross sections, giving an accurate value of the thermal integral using a computationally feasible number of trajectories. The most important feature of the present technique is that it appears possible to evaluate the thermal integral over a considerable temperature range for only one set of trajectory calculations. It is this feature which makes parametric investigation of the potential parameters, an essential aspect of the analysis, appear feasible.

While the Monte Carlo method of Section 3 has been developed for the present vibrational excitation calculations, wider applications appear promising. Calculation of thermal transport coefficients and high-activation-energy reactive scattering cross sections are two such possibilities.

The four-body, exact classical analysis reported in Section 4 has been developed primarily to investigate the range of validity of the decoupled normal mode model of Section 2. The four-body analysis, however, will provide a flexible tool for investigation of the classical trajectories involving linear triatomics. In particular, study of dissociative scattering with this program will be possible.

The studies reported in Section 5 utilize greatly simplified collision models to obtain analytic expressions for the vibrational transition probabilities. These analyses have served as a guide in developing the thermal averaging calculations of Section 3. They provide easily-evaluated transition probability expressions, which give qualitatively correct dependence on trajectory parameters.

An anharmonic CO_2 model is described in Section 6, although calculations with this model have not been performed as yet. Transition probabilities to be obtained from such calculations should be of considerable interest for understanding of CO_2 gas laser processes. For example, deactivation of the lower laser level (100°) to the (02°0) state by collision is an important intramolecular V-V process.[20] These are two states mixed by Fermi resonance coupling, with a resonance defect of only 102 cm^{-1}. It is therefore expected that the probability for this collisionally induced transition will be quite large. The only previous theoretical prediction of this probability is the distorted wave calculation of Herzfeld,[11] who predicts a value of 3.5×10^{-3} for the transition probability at room temperature for CO_2 - CO_2 collisions. Comparison with results obtained using the multistate calculation of Section 6 will add to understanding of these processes.

APPENDIX A
RIGID ROTATOR-ATOM EQUATIONS OF MOTION

The classical equations of motion for the collision of a rigid triatomic rotator model of CO_2 with an atom were programmed for numerical integration using a Runge-Kutta scheme. The equations, as programmed in dimensionless form, using the notation of Figs. 1-2, are:

$$\frac{d\alpha}{d\tau} = \frac{\hat{P}_\alpha}{\sin^2\beta} \tag{A-1}$$

$$\frac{d\beta}{d\tau} = \hat{P}_\beta \tag{A-2}$$

$$\frac{d\hat{R}}{d\tau} = \hat{P}_R \tag{A-3}$$

$$\frac{d\Theta}{d\tau} = \frac{\hat{P}_\Theta}{\hat{R}^2} \tag{A-4}$$

$$\frac{d\Phi}{d\tau} = \frac{\hat{P}_\Phi}{\hat{R}^2 \sin^2\Theta} \tag{A-5}$$

$$\frac{d\hat{P}_\alpha}{d\tau} = -\frac{\partial\hat{V}}{\partial\alpha} \tag{A-6}$$

$$\frac{d\hat{P}_\beta}{d\tau} = \frac{\hat{P}_\alpha^2 \cot\beta}{\sin^2\beta} - \frac{\partial\hat{V}}{\partial\beta} \tag{A-7}$$

$$\frac{\partial\hat{P}_R}{\partial\tau} = \frac{1}{\hat{R}^3}\left[\hat{P}_\Theta^2 + \hat{P}_\Phi^2 \sin^{-2}\Theta\right] - \frac{\partial\hat{V}}{\partial\hat{R}} \tag{A-8}$$

$$\hat{P}_{\Phi} = \hat{M}_z - \hat{P}_{\alpha} \tag{A-9}$$

$$\hat{P}_{\Theta} = \tan\Phi \cot\Theta \hat{P}_{\Phi} + \sin\alpha \cot\beta \sec\Phi \hat{P}_{\alpha} - \cos\alpha \sec\Phi \hat{P}_{\beta} + \hat{M}_y \sec\Phi \tag{A-10}$$

Equations (A-1) - (A-8) are in the Hamilton's form; in Eqs. (A-9) and (A-10), conservation of total angular momentum about the z and y axes has been used to eliminate the differential relation in $\hat{P}_{\Phi}$ and $\hat{P}_{\Theta}$. The angular momenta are evaluated initially, being given by:

$$\hat{M}_y = -\sin\Phi \cot\Theta \hat{P}_{\Phi} + \cos\Phi \hat{P}_{\Theta} - \sin\alpha \cot\beta \hat{P}_{\alpha} + \cos\alpha \hat{P}_{\beta}$$

$$\hat{M}_z = \hat{P}_{\Phi} + \hat{P}_{\alpha}$$

Conservation of angular momentum about the x axis and also of the total Hamiltonian are reserved as checks on the numerical computation:

$$\hat{M}_x = -\cos\Phi \cot\Theta \hat{P}_{\Phi} - \sin\Phi \hat{P}_{\Theta} - \cos\alpha \cot\beta \hat{P}_{\alpha} - \sin\alpha \hat{P}_{\beta} \tag{A-11}$$

$$= \text{const}$$

$$\hat{H} = \frac{1}{2}\hat{P}_{\beta}^2 + \frac{1}{2}\hat{P}_{\alpha}^2 \sin^{-2}\beta + \frac{1}{2}\hat{P}_R^2 + \frac{1}{2\hat{R}^2}\hat{P}_{\Theta}^2 + \frac{1}{2\hat{R}^2 \sin^2\Theta}\hat{P}_{\Phi}^2 + \hat{V} \tag{A-12}$$

$$= \text{const}$$

Also

$$\frac{\partial \hat{V}}{\partial \alpha} = -\hat{\ell} \sin\beta \sin\Theta \sin(\alpha - \Phi) S$$

$$\frac{\partial \hat{V}}{\partial \beta} = -\hat{\ell}\left[\sin\beta\cos\Theta - \cos\beta\sin\Theta\cos(\alpha-\Phi)\right] S$$

$$\frac{\partial \hat{V}}{\partial \hat{R}} = -\hat{\alpha}_1 \hat{C}_1 e^{-\hat{\alpha}_1\hat{R}} + \hat{\alpha}_4 \hat{C}_4 e^{-\hat{\alpha}_4\hat{R}} - \hat{\alpha}_2 \hat{C}_2 \hat{R}\left[e^{-\hat{\alpha}_2\hat{\xi}_2}/\hat{\xi}_2 + e^{-\hat{\alpha}_2\hat{\xi}_3}/\hat{\xi}_3\right]$$

$$+ \frac{\hat{\ell}}{\hat{R}}\left[\cos\beta\cos\Theta + \sin\beta\sin\Theta\cos(\alpha-\Phi)\right] S$$

where

$$S = \hat{\alpha}_2 \hat{C}_2 \hat{R}\left[e^{-\hat{\alpha}_2\hat{\xi}_2}/\hat{\xi}_2 - e^{-\hat{\alpha}_2\hat{\xi}_3}/\hat{\xi}_3\right]$$

$$\hat{\xi}_2 = \left\{\hat{R}^2 + \hat{\ell}^2 - 2\hat{\ell}\hat{R}\left[\cos\beta\cos\Theta + \sin\beta\sin\Theta\cos(\alpha-\Phi)\right]\right\}^{1/2}$$

$$\hat{\xi}_3 = \left\{\hat{R}^2 + \hat{\ell}^2 + 2\hat{\ell}\hat{R}\left[\cos\beta\cos\Theta + \sin\beta\sin\Theta\cos(\alpha-\Phi)\right]\right\}^{1/2}$$

The nondimensionalization used is

Characteristic Length: $\sqrt{I/M}$

Characteristic Mass: M

Characteristic Time: $\sqrt{I/M}/V$

where V is a characteristic velocity to be specified, I is the moment of inertia, and M is the reduced mass for CO_2-M collisions. Then

$\hat{P}_\alpha = \dfrac{P_\alpha}{V\sqrt{MI}}$, and a similar arrangement applies for $\hat{P}_\beta$, $\hat{P}_\theta$, $\hat{P}_\Phi$, M_x , M_y , M_z .

$\hat{P}_R = \dfrac{P_R}{MV}$

$\hat{R} = \dfrac{R}{\sqrt{I/M}}$

$\hat{M} = 1$

$\hat{V} = \dfrac{V}{MV^2}$

$$\hat{C}_1 = C_1/MV^2 , \quad \hat{C}_2 = C_2/MV^2 , \quad \hat{C}_4 = C_4/MV^2$$

$$\hat{\alpha}_1 = \alpha_1\sqrt{I/M} , \quad \hat{\alpha}_2 = \alpha_2\sqrt{I/M} , \quad \hat{\alpha}_4 = \alpha_4\sqrt{I/M}$$

$$\hat{l} = \frac{l}{\sqrt{I/M}}$$

$$\hat{\zeta}_2 = \zeta_2/\sqrt{I/M} , \quad \hat{\zeta}_3 = \zeta_3/\sqrt{I/M}$$

Initial conditions are based on the orientation of Fig. 11:

$$\alpha_o$$

$$\beta_o$$

$$\Phi_o = \sin^{-1}\left(\frac{b}{R_o}\right)$$

$$\Theta_o = \pi/2$$

$$\hat{R}_o = R_o/\sqrt{I/M}$$

$$\hat{P}_{\alpha_o} = \omega_{\alpha_o}\frac{\sqrt{I/M}}{V}$$

$$\hat{P}_{\beta_o} = \omega_{\beta_o}\frac{\sqrt{I/M}}{V}$$

$$\hat{P}_{\Phi_o} = \left(\frac{V_\infty}{V}\right)\left(\frac{b}{\sqrt{I/M}}\right)$$

$$\hat{P}_{\Theta_o} = 0$$

$$\hat{P}_{R_o} = -\left(\frac{V_\infty}{V}\right)\cos\Phi_o = -\left(\frac{V_\infty}{V}\right)\left(1-\frac{b^2}{R_o^2}\right)^{1/2}$$

Constants to be read in:

$$I,\ M,\ V,\ C_1,\ C_2,\ C_4, \alpha_1, \alpha_2, \alpha_4$$

Initial condition parameters to be read in:

$$\alpha_o ,\ \beta_o ,\ R_o ,\ \omega_{\alpha_o} ,\ \omega_{\beta_o} ,\ V_\infty ,\ b$$

APPENDIX B
VIBRATIONAL DISPLACEMENTS

We refer to Fig. 12 and the definitions of S_1 , S_2 , S_3 given on page . The molecular axis is defined as the line parallel to the O-O internuclear distance that passes through the molecular c. m.* Using the definitions of $\bar{Q}_{j+3} = Q_4 \hat{\imath} + Q_5 \hat{\jmath} + Q_6 \hat{k}$ and $\bar{Q}_{j+6} = Q_7 \hat{\imath} + Q_8 \hat{\jmath} + Q_9 \hat{k}$ given on page , we see the following geometrical relations between $\bar{Q}_{j+3}$, $\bar{Q}_{j+6}$ and S_1 , S_2 , S_3 :

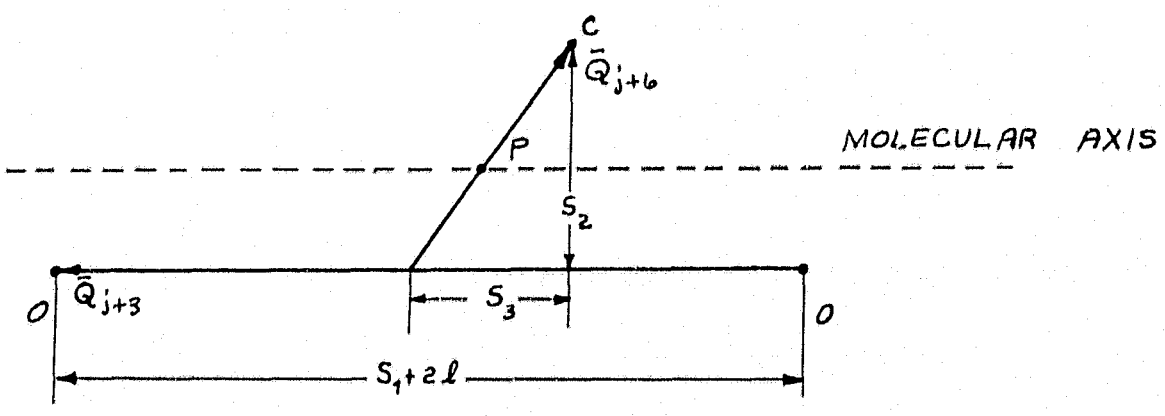

From the figure

$$S_1 + 2\ell = \left| \bar{Q}_{j+3} \right| = \sum_{j=1}^{3} \left[Q_{j+3}^2 \right]^{1/2}$$

$$S_2 = \left| \bar{Q}_{j+6} \times \bar{Q}_{j+3} \right| \Big/ \left| \bar{Q}_{j+3} \right|$$

$$= \left| \bar{Q}_{j+3} \right|^{-1} \begin{vmatrix} \hat{\imath} & \hat{\jmath} & \hat{k} \\ Q_7 & Q_8 & Q_9 \\ Q_4 & Q_5 & Q_6 \end{vmatrix}$$

*This special definition serves for describing the normal vibrational displacements in CO_2.

$$= |\bar{Q}_{j+3}|^{-1} \left| (Q_6 Q_8 - Q_5 Q_9)\hat{i} - (Q_6 Q_7 - Q_4 Q_9)\hat{j} + (Q_5 Q_7 - Q_4 Q_8)\hat{k} \right|$$

$$= |\bar{Q}_{j+3}|^{-1} \left[(Q_6 Q_8 - Q_5 Q_9)^2 + (Q_6 Q_7 - Q_4 Q_9)^2 + (Q_5 Q_7 - Q_4 Q_8)^2 \right]^{1/2}$$

$$S_2 = \frac{\left[(Q_6 Q_8 - Q_5 Q_9)^2 + (Q_6 Q_7 - Q_4 Q_9)^2 + (Q_5 Q_7 - Q_4 Q_8)^2 \right]^{1/2}}{\left[Q_4^2 + Q_5^2 + Q_6^2 \right]^{1/2}}$$

ξ

$$S_3 = \bar{Q}_{j+6} \cdot \bar{Q}_{j+3} \Big/ |\bar{Q}_{j+3}|$$

$$S_3 = (Q_4 Q_7 + Q_5 Q_8 + Q_6 Q_9) \Big/ (Q_4^2 + Q_5^2 + Q_6^2)^{1/2}$$

In the initial orientation of the molecule, as described on page , the molecule is confined to the zy plane, so all x displacement components are zero, $Q_4 = Q_1 = 0$. Also, the y axis is parallel to the 0-0 line, so that $Q_6 = 0$. Thus, the above relations reduce to

$$\left.\begin{aligned} S_1 &= Q_5 - 2\ell \\ S_2 &= Q_9 \\ S_3 &= Q_8 \end{aligned}\right\} \quad \text{initially}$$

REFERENCES

1. Rapp, D., and Kassal, T., "A Review of the Theory of Vibrational Energy Transfer between Simple Molecules in Nonreactive Collisions," Grumman Research Dept., Rept. RE-345, Grumman Aircraft Engineering Corp., Bethpage, New York, Oct. 1968.
2. Borrell, P., Adv. in Molecular Relaxation Processes, I, 69 (1967).
3. Treanor, C.E., J. Chem. Phys. 43, 532 (1965).
4. Benson, S.W. and Berend, G.C., J. Chem. Phys. 44, 4247 (1966).
5. Sharp, T.E. and Rapp, D., J. Chem. Phys. 43, 1233 (1965).
6. Mies, F.H., J. Chem. Phys. 42, 2709 (1965).
7. Takayanagi, K., Progr. Theoret. Phys. (Kyoto) Suppl. No. 25, 1 (1963).
8. Takayanagi, K., Adv. in Atomic and Molecular Phys. 1, 149 (1965).
9. Kuksenko, B.V., et al., Dokl. Akad. Nauk SSSR 167, 6, 1280 (1966).
10. Mott, N.F., and Massey, H.S., The Theory of Atomic Collisions, 3rd Ed., Oxford Univ. Press (1965).
11. Herzfeld, K.F., J. Chem. Phys. 47, 743 (1967).
12. Marriott, R., Proc. Phys. Soc. 88, 83 (1966).
13. Witteman, W.J., J. Chem. Phys. 35, 1 (1961).
14. Shields, F.D. and Burks, J.A., J. Acoust. Soc. Am. 43, 510 (1968).
15. Kuksenko, B.Y. and Losev, S.A., Sov. Phys.-Dokl. 13, 142 (1968).
16. Karplus, M. and Raff, L.M., J. Chem. Phys. 41, 1267 (1964).
17. Raff, L.M., J. Chem. Phys. 44, 1202 (1966).
18. Houghton, J.T., Proc. Phys. Soc. 91, 439 (1967).
19. Yardley, J.T. and Moore, C.B., J. Chem. Phys. 46, 4491 (1967).

20. Taylor, R. L. and Bitterman, S., "Survey of Vibrational Relaxation Data for Processes Important in the CO_2-N_2 Laser System," Avco Everett Research Laboratory Rept. 282 (Oct. 1967).

21. Rose, M. E., Elementary Theory of Angular Momentum, John Wiley and Sons, Inc., London, 1957.

22. Herzberg, G., Molecular Spectra and Molecular Structure II, Infrared and Raman Spectra of Polyatomic Molecules, D. Van Nostrand Co., Inc., Princeton, 1945.

23. Parker, J. G., Phys. Fluids 2, 449 (1959).

24. Raff, L. M., J. Chem. Phys. 46, 520 (1967).

25. Rapp, D., J. Chem. Phys. 32, 735 (1960).

26. Cottrell, T. L., and McCoubrey, J. C., Molecular Energy Transfer in Gases, Chap. 6, Butterworths, London, 1961.

27. Kerner, E., Can. J. Phys. 36, 371 (1958).

28. Hirschfelder, Curtiss, and Byrd, Molecular Theory of Gases and Liquids, John Wiley & Sons, New York, 1954.

29. Schreider, Yu. A. (ed.), Method of Statistical Testing, Monte Carlo Method, Chaps. 1 and 2, Elsevier Publishing Co., New York, 1964.

30. Hammersley, J. M. and Handscomb, D. C., Monte Carlo Methods, Chap. 5, John Wiley & Sons, Inc., New York, 1964.

31. Cross, R. J., and Herschbach, D. R., J. Chem. Phys. 43, 3530 (1965).

32. Nikitin, E. E., Optics and Spectroscopy VI, 93 (1959).

33. Takayanagi, K., J. Phys. Soc. Japan 14, 75 (1959).

34. Salkof, M. and Bauer, E., J. Chem. Phys. 29, 26 (1958).

35. Raff, L. M., J. Chem. Phys. 46, 520 (1967).

36. Lordi, J. A., Dissertation, State Univ. of New York at Buffalo, 1968.

37. Rapp, D., and Sharp, T. E., J. Chem. Phys. 38, 2641 (1963).

38. Dennison, D. M., Phys. Rev. 41, 304 (1932).

39. Adel, A., and Dennison, D. M., Phys. Rev. 43, 716; 44, 99 (1933).

40. Sharp, T. E., and Rapp, D., J. Chem. Phys. 43, 532 (1965).